Energy Equip. Sys./ Vol. 12/No. 4/December 2024/ 341-377

ENERGY EQUIPSYS

Energy Equipment and Systems

www.energyequipsys.com

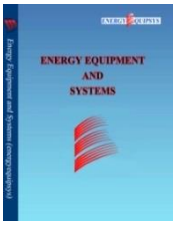

Multi-objective optimization of air conditioning systems in residential buildings with an economic attitude

Manuscript Type
Research Paper

Authors

Afshin Ahmadi Nadooshan[a*]
Seyed Amir Hossein Hashemi Dehkordi[a]
Morteza Bayareh[a]
Mohammadreza Baghoolizadeh[a]
Dariush Bahrami Eisaabadi[b]

[a] Department of Mechanical Engineering, Shahrekord University, Shahrekord 88186-34141, Iran

[b]Chemical Engineering and Industrial Chemistry, Faculty of Engineering, Vrije Universiteit Brussel, Belgium

ABSTRACT

The development of life over successive years causes an increasing consumption of energy consumption; the same factor causes people to face energy consumption. The use of fossil fuels for energy supply causes air pollution and environmental degradation factors, which itself causes climate change in the world. Therefore, researchers are looking for ways to optimize energy consumption in the world. One of these ways is to optimize the energy consumption of air conditioners in buildings. For this purpose, this study demonstrates that optimizing the amount of energy consumption of air conditioning systems (ACS) in a residential building helps significantly in reducing the energy consumption of the building. For this purpose, six residential buildings in 4 cities of Iran (Tehran, Shahrekord, Rasht and Bandar Abbas) with different climates have been investigated. For this purpose, 5 design variables of summer clothing insulation level (SCIL), winter clothing insulation level (WCIL), ACS (40 different ACS), cooling thermostat temperature (CTT) and heating thermostat temperature (HTT) have been considered. The objective functions in this study are the cost of installing the air conditioning system (CIACS), the annual cost of bills (ACB) and the predicted percentage of dissatisfied (PPD). The effect of design factors on objective functions has been investigated by Morris's sensitivity analysis. Three Energy Plus, JEPLUS and JEPLUS+EA software are used for optimization. For this purpose, non-dominant sorting genetic algorithm (NSGA-II) - is used for optimization. The optimization results after the calculations showed that Tehran's annual energy consumption has decreased by 81.3%, Rasht by 63.64%, Bandar Abbas by 82.66% and Shahrekord by 77.2%. Also, the PPD for the cities of Tehran, Rasht, Bandar Abbas and Shahrekord improved by 44.42, 50.1, 31.1 and 56.3% respectively.

Article history:
Received : 15 April 2024
Revised: 11 August 2024
Accepted : 9 September 2024

Keywords: PPD, ACS, ACB, CIACS, NSGA-II.

[*] Corresponding author: Afshin Ahmadi Nadooshan
Department of Mechanical Engineering, Shahrekord University, Shahrekord 88186-34141, Iran.
Email: ahmadi@sku.ac.ir

1. Introduction

1.1. Energy problem

In recent ages, the amount of inappropriate energy consumption that has occurred throughout human history has led to worldwide issues and, ultimately, an environmental disaster. Thus, between 2012 and 2040, the energy used in residential, commercial, and industrial buildings will account for 1.20 percent of the world's total energy consumption. Additionally, a 750% rise in energy consumption is expected for the Asian continent. About 25 to 30 percent more carbon dioxide is released into the atmosphere as a result of this increase in energy consumption [1, 2]. As a result, modern buildings' efficient designs can significantly contribute to a decrease in global energy usage. The kind of heating, and cooling ACS in residential and commercial buildings have a significant impact on energy efficiency; by optimizing these systems, up to 50% of the building's total energy usage may be reduced [3]. The International Energy Agency data indicate that overall investment in commercial, residential, and industrial building energy efficiency has grown and is expected to reach 125 billion dollars in the next three years [4]. Additionally, commerce in ACS has grown from 86.6 billion dollars in 2012 to 97.9 billion dollars in 2014 on the worldwide market [5]. By focusing on this crucial aspect of buildings, engineers and researchers have been able to come up with solutions for lowering energy usage in both commercial and residential structures. One of these ways is to optimize the building's ACS.

1.2. Literature Review on ACS

Léger et al.'s study [6] examined three electric heaters that used various kinds of specialty thermostats to provide thermal comfort. They performed a continuous calculation of the output values for the room at +10, 0, -10, and -20 degrees Celsius. Based on the collected data, they concluded that not all electric heaters use the same amount of energy and that each one's efficiency varies depending on how its components are arranged and how its blades radiate. Aktacir et al. [7] investigated three distinct building types in the hot and muddy city of Adana, Türkiye. They looked into the upfront costs associated with installing and buying ACS for both variable and fixed air volume systems. The acquired findings demonstrated a 22% reduction in the system's startup cost, a 25% reduction in the cost of operating the fixed air volume system, and a 33% reduction in the cost of operating the variable air volume system. Cen et al. [8] employed a floor radiant radiator system for winter heating and a fan coil system for summer cooling in residential buildings located in Tianjin, China, to perform an extensive study on the thermal comfort of occupants at different heights in a particular area. Generally, the sensory questionnaire was completed by 30 subjects who were examined in 8 distinct experimental setups. They concluded that there were notable differences between the fan coil systems and radiation from the floor's operating temperature and thermal comfort for spaces of the same height. Additionally, they found that the fan coils' neutral temperature decreased with height while the system's neutral temperature increased due to floor radiation. In a study conducted by Pandelidis et al. [9], the combined performance of an air conditioning system with new evaporative cooling in buildings situated in temperate and favorable climates was examined. Building energy simulations were used to compute the yearly data conditions for the quantity of air required and the associated energy consumption. Tewari et al. [10] gathered 1554 distinct data points for their study of the thermal comfort of ten distinct residential structures in India over several years. These values were computed utilizing an evaporative cooling air conditioning system in various Indian climes for various age groups and clothing covering levels. They were able to find the ideal condition between the parameters by employing linear regression between the data, and 86% of subjects felt thermally comfortable and at ease at 28.2 degrees Celsius. In four Iranian climates, Naderi et al.'s study [11] examined the impact of direct evaporative cooling system characteristics. The saturation temperature efficiency of the pads, the volume of airflow, and the exact thermostat control points of the air conditioning system are the criteria they establish as their targets. They discovered that using a direct evaporative cooling system resulted in lower power and higher water use and that it provided more

accurate adjustments to thermal comfort and air humidity than packaged ACS did. To improve a building's energy usage, Yu et al. [12] simultaneously investigated two variable air volume systems and variable refrigerant flow systems in China. The results showed that variable refrigerant flow systems use up to 70% less energy than variable air volume systems, and that variable refrigerant flow systems use a significant reduction in energy consumption over variable air volume systems. An integrated solid dehumidifier with variable refrigerant flow was presented by Jiang et al. [13] in a novel heat pump system module.

Furthermore, they examined and computed summer and winter performance coefficients and energy consumption in terms of EnergyPlus software's efficiency capability. They discovered that the solid dehumidifier heat pump operates best in summer and has a more tolerable capacity in winter, depending on the humidity ratio and ambient temperature. As the heat ratio increased, they discovered that the device's efficiency dropped. Song et al.'s study [14] used a packaged air conditioning system to study thermal comfort in a university setting. To find out when students used the air conditioning, a sample of 25 students was chosen for the study. Every minute, they monitored the ambient temperature and relative humidity at a distance of 75 cm from the ground surface while conducting a regular discourse. The measurements were taken once with the air conditioner on and twice without it. Data were gathered without the use of air conditioning. They also looked at the average impact of airspeed and people's garment surface, and the findings showed that it would need more energy to achieve temperatures between 23.7 and 27.4 degrees Celsius. The average temperature of the skin rises from 32.1 to 32.7 degrees Celsius when the air conditioner is switched off. They were able to maintain the kids' thermal comfort in the most precise and efficient manner by optimizing the data. Aynur et al. [15] modeled an air conditioning system with variable air volume in a building for air conditioning mode using Energy Plus, an energy analysis program. They discovered that 71.1% of the total power usage was approximated by modeling this air conditioning system in Energy Plus software, together with its interior temperature and relative air humidity. This is within 15% of the experimental data. It is possible to maintain, optimize, and keep the temperature within the building's rooms at 65.8% with the variable air volume system operating correctly in terms of energy exchange and internal temperature. Additionally, it was shown that variable refrigerant flow offers superior thermal comfort performance. The topic of temperature control for air cooling with a variable refrigerant system or variable refrigerant flow system was covered by Moon et al. [16]. To improve the thermal comfort of the building's inhabitants, they introduced a new control algorithm that takes into account the quantity of indoor environment, air humidity, and the building's initial indoor air quality when the air conditioning system is installed. They also looked at how well this new algorithm performed in terms of thermal comfort ratio and energy usage. They discovered that when the temperature setting is changed, the thermal comfort management algorithm uses around 10% more energy on hot and muggy days. For almost 95% of the procedure, thermal comfort is maintained. Furthermore, this algorithm uses more energy on days that are moderate and hot, yet it still results in thermal comfort for over 98% of users. Zhang et al.'s [17] study focused on the precise heat recovery configurations in industry and academia using variable refrigerant flow systems. To replicate the energy use of the air conditioning system with far more sophisticated management, they unveiled a new model. Additionally, these researchers thoroughly assessed this system using the Energy Plus program, and they discovered that buildings with this kind of system function better and are more dynamic than those with laboratory mode. Four distinct kinds of pads used in evaporative cooling systems were examined by Nada et al. [18]. The amount of air temperature drop, the amount of air humidity increase, the amount of cooling capacity, the rate of water evaporation over time, and the energy consumed in the total time efficiency were all factors they looked at while testing the cooling pad. They made the payment. The impacts of airspeed, inlet air temperature, water flow rate, water temperature, and cooling pad thickness on all of these performance factors were examined and studied by these researchers. The energy efficiency and thermal comfort of a fan coil air conditioning system were examined by Chu et al. [19]. To precisely and promptly regulate the fan coil of the single-phase control unit, they looked

at the ratio of thermal comfort to the surface and once used the enthalpy theory. This research aims to keep the occupants' thermal comfort level at an acceptable level. It was a structure. Using an evaporative cooling system, Bishoyi et al. [20] looked at the cooling load, power usage, and energy efficiency ratio. They conducted both analytical and experimental follow-ups on their study. They discovered that an evaporative cooler with a honeycomb cooling pad has a significantly higher ratio of energy efficiency and cooling capacity than a conventional Aspen cooling pad with the same surface area. They also discovered that using these honeycomb cooling pads in hot, arid conditions, a beehive is far more appropriate than push pads. The amount of energy loss in the control unit of a variable air volume system in a building was examined by Deshmukh et al. [21]. They concluded that buildings account for more than 40% of the country's yearly energy use. They looked at the ventilation systems' leaks and their flows to learn more and salvage more in this instance. These Boston-area researchers were able to reduce expenses by 18%, or more than $340 a month, after gathering data and identifying systemic problems. Additionally, they achieved improved productivity with more precise monitoring and the usage of various sensors, resulting in a $500, or 2.5%, cost savings by minimizing the amount of air leakage associated with the dampers. MARTíNEZ et al.'s [22] experimental study looked at how the heat pump's packaged air conditioning system may reduce energy use and improve its refrigeration performance coefficient by employing several kinds of pads with varying thicknesses and condenser pre-cooling. Through their ability to lower the condenser's intake temperature and pressure throughout the refrigeration cycle, they were also able to lower the amount of power consumed. Additionally, they discovered that adiabatic pads are ineffective in extremely humid environments and that their design requires additional components, increasing the device's cost and dimensions. In Jaipur city, Tewari et al. [23] looked into ten office buildings. In comparison to other conventional systems, they were able to give office building occupants more thermal comfort throughout the summer by utilizing the evaporative cooling system, also known as the evaporative cooler. In their investigation and analysis of the cornice-type radiator, Gheibi et al. [24] also offered a design that improves thermal efficiency by rearranging the fins and their geometry and enlarging the tube diameter. By examining the thermal comfort of the occupants, these experts were able to improve the air conditioning system's effectiveness by 32% when compared to radiators that had the original design. Through the use of Energy Plus software to simulate building energy use, Yun et al. [25] evaluated a variable refrigerant flow system. According to the study findings, the goal function should be used to estimate the performance of the variable refrigerant flow system. The simulation results indicate that the cooling system's yearly energy consumption is lowered by 14%. The type of insulation used in a refrigerant variable flow system with high energy savings and cost repayment over ten years was examined by Yildiz et al. [26]. They discovered that the air conditioning system requires an insulation thickness of between 16 and 20 mm for high-pressure pipes in the heating mode, 11 to 13 mm for low-pressure pipes, and 7 to 8 mm for the cooling mode. In commercial buildings with variable air volume systems, Krishnamoorthy et al. [27] looked at the assessment of energy losses from duct air leakage during central heating and outdoor air cooling. To achieve this, the cooling needs of buildings and the amount of external air preheating in Chicago, California, and Sacramento were calculated without any duct leaks. that the level of leakage from the steel channel was examined between 9.8 and 27.8%, and that their air ratio in the open space was independently adjusted between 10 and 30%. It is evident from their findings that the air conditioning system in the city of California has very little influence on the loads for heating and cooling. Based on an economizer cycle and an enthalpy-based cycle, Yao et al. [28] examined the variable air volume air conditioning system in a Chinese office building locally in six climatic points with two types of temperatures. They concluded that the ventilation system in the hot and humid southern region of China performs significantly better in terms of energy conservation than the system in the northern region and that the enthalpy-based cycle design outperforms the economizing cycle type in hot and humid conditions. Cho et al. [29] examined numerical data in split box control algorithms to enhance thermal conditions and reduce energy consumption in a Chinese building's air

conditioning system that used a variable air conditioning system. These scientists discovered that in atypical environmental circumstances, energy consumption may be decreased by maintaining a steady temperature.

1.3. Literature Review on Optimization

Owing to time constraints and administrative constraints during scientific experimentation and data extraction, researchers were compelled to develop procedures that would yield findings faster and with a reduced error rate. As a result, they started using machine algorithms, which call for the random sampling technique to get quantitative experimental data [30-46]. The algorithm's objectives are assessed using this data. Finding the best solutions is usually quite challenging and may even stray from the intended course since machine learning and optimization algorithms are now more effective. Common techniques for optimizing energy use include the use of software like GENOPT, jEPlus + EA, etc. These applications are composed of several genetic algorithm-based plugins, such as Ladybug and Honeybee. One of the best techniques for dealing with energy-related problems in buildings is this algorithm. Among these, the energy optimization is quite accurate and the JEPLUS+EA program pairs well with the EnergyPlus software. Kerdan et al. [47] used neural network optimization to study the cost cycle and inhabitants' thermal comfort in a historic building across three distinct temperature zones in Mexico. They were able to optimize the building's thermal comfort, energy use, and power costs by more than 95% by employing neural network optimization. Using a multi-purpose genetic algorithm model, Markarian et al. [48] minimized the heating and cooling load of a four-story structure in five distinct climates of Iran, including Tehran, Tabriz, Bandar Abbas, Shiraz, and Yazd. The system was a heat pump packaged air conditioning system. Researchers have looked into several phase-change materials to lower the quantity of carbon dioxide required for energy production. Phase-changing materials have decreased yearly carbon dioxide emissions for Tehran, Tabriz, Bandar Abbas, Shiraz, and Yazd, respectively, and electrical energy consumption for all climates between 4.5 and 5.5%. There has been a reduction in 1297 kg, 1420 kg, 2040 kg, 1027 kg, and 1248 kg. Additionally, it will take around 70 years to recover the expenses of undertaking this operation in all climates. Baghoolizadeh et al.'s [33] study looked at how to best use a solar canopy to produce power while consuming less energy. With the use of Energy Plus software, they evaluated and replicated a particular structure for five locations around Europe. Additionally, they used the JEPLUS+EA algorithm to determine the best angle to take to generate electricity with the highest efficiency while preserving ambient lighting and thermal comfort in these cities. This allowed them to use the multi-objective optimization method to identify the ideal scenario. The specialized outside air system and the variable refrigerant flow system were examined and assessed by Kim et al. [49]. To do this, they created a strategic multi-purpose control in Energy Plus software that maximizes air humidity, thermal comfort, and energy usage. By utilizing the genetic algorithm, they managed to decrease the overall energy usage by 20.4% and enhance thermal comfort by 19.1%. Energy Plus software and the MATLAB genetic algorithm were used by Lee et al. [50] to investigate the variable air volume system in a South Korean office building. They discovered that this kind of algorithm may be used to conserve energy in forced ACS and can drastically lower energy usage. Xu et al. [51] talked about the variable air conditioning system-based air conditioning rate management technique, which improved the building's indoor air quality, allowed for more natural light to enter the area, provided thermal comfort, and maximized energy use. The genetic algorithm was utilized to compute these variables, and the cost function was chosen for this investigation based on their values. Additionally, they presented the optimal energy consumption optimization for each climatic zone. Baghoolizadeh et al.'s study [52] looked at the smart shade's functionality and architectural features of the structure. They assessed the cooling and heating loads brought on by sunshine entering a building by modeling this smart shade. They then used soft JEPLUS+EA software to do multi-objective optimization on the shade angle. Using multi-objective optimization of the genetic

algorithm, the researchers in this study were able to reduce the building's annual energy consumption by 40–50% by altering the shade's angle, location, and material composition while still preserving Tehran's PPD. The quantity of carbon dioxide produced in five American cities was examined by Baghoolizadeh et al. [53]. They began by looking into the components that cause the heat pump ACS to produce carbon dioxide. Next, they used JEPLUS+EA software or a multi-objective genetic algorithm to adjust the thermostat's temperature and check the system's heating and cooling capabilities as well as the amount of the employees' attire allowed for the identification of the best mode for each climate and the reduction of the building's carbon dioxide emissions.

1.4. Aim and study

Most of the studies conducted by researchers and scientists have focused on a specific type of ACS, and they have also examined these systems in only one city. In this study, the aim is to simulate common ACS in Iran in different climates. For this purpose, in this study, fan coil ACS, Packaged Terminal Heat Pump (PTHP), radiator and evaporative cooler combinations, Packaged Terminal Air Conditioning (PTAC), and Variable Refrigerant Flow (VRF) systems have been used, which have been used in different capacities for diversity. Finally, 40 types of ACS have been selected. The studied cities are Tehran, Shahrekord, Rasht, and Bandar Abbas. To select the optimal ACS, an optimization method was used, which used the combination of three Energy Plus software programs, jEPLUS and jEPLUS +EA. For this purpose, the design variables are the type of ACS, the temperature of the heating and cooling thermostat, as well as the clothing level of the winter and summer residents. The goal is to optimize the CIACS, and the ACB (water, electricity, and gas), and improve PPD. Therefore, the objectives of this study can be categorized as follows.

- Studying 4 different types of climates in Iran and choosing the air conditioning system suitable for their conditions.
- Simulation of PTHP, PTAC, VRF, radiator and evaporative cooler air conditioning systems based on their specifications and catalog.
- Economic optimization of ACB and CIACS along with PPD.
- Examining study parameters by Morris sensitivity analysis.

2. Validation

Given that this investigation was conducted numerically rather than experimentally, a comparison with an experimental study is made to verify the findings obtained using the energy modeling program EnergyPlus. In 2018, Fathalian et al. [54] conducted their studies on the three-story building of the Gas Department in Semnan. First, they simulated the office building inside the Design Builder software, then calculated the amount of heating and cooling energy in the building, and finally compared the data with the actual consumption values. In this study, they used a heater for the heating system and a spilled for the cooling system, which corresponds to the ACS of the Iranian office building. Because the real system was used in the study of Fath Aliyan et al. and due to the similarity of this study with the present study, this study is therefore used for validation. In this study, to validate, the mentioned building has been modeled, and the output data has been compared with the actual values of energy consumption. Therefore, the existing three-story office building in Semnan City has been modeled with all its details in the modeling software. For example, the modeling of the building shell, including walls, ceilings, floors, glass, window frames, and doors, as well as the type of arrangement of their layers and the physical values of their properties, such as density, thermal conductivity coefficient, thickness, etc., are entered into the software by the data values of the study by Fathalian et al. [54]. After modeling the building, the output of the software was transferred to the Energy Plus software, and this time the heating and cooling ACS were simulated to calculate the energy consumption of the building in cold and hot months. The simulated building can be seen in Fig. 1, as well as the comparison of the simulation results and the experimental study of Fathalian et al.[54] in Table 1.

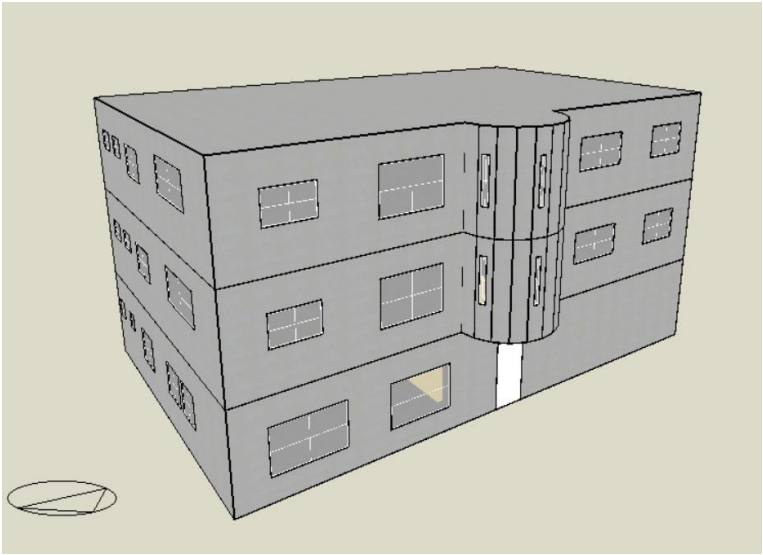

Fig. 1. The building is simulated in the software.

Table 1. Comparison of building energy consumption in two experimental [54] and numerical modes.

	Energy consumption by experimental (kWh)	Energy consumption by EnergyPlus (kWh)	Error percentage (%)
Cooling	23649	23350.18	1.27
Heating	77784	74415.31	4.33
Total	101433	97765.49	3.62

The results show that the simulation data is close to the real data and its error is less than 5%, which is acceptable for validation.

3. Methodology

3.1. Climate

As seen in Fig. 2, the areas of Iran are classified into four climates according to Pourvahidi et al.'s [55] classification of climates. Consequently, a large city is selected to represent each current environment and is employed in the study for each climate. Fig. 2 illustrates Tehran's geographic position, which lies south of the Alborz Mountain range. Tehran has hot, dry summers and cold, dry winters as a result of its geographic location. Because Bandar Abbas is situated close to the sea on the south and the desert on the north, it experiences greater temperatures and humidity levels than other parts of the country. This results in a hot and humid (tropical) climate. Winters in Bandar Abbas are shorter and milder than those in Tehran. In contrast, Shahrekord has a chilly climate because of its high elevation about other Iranian towns and its location in the Zagros Mountain range. This city experiences longer, extremely cold winters, and its summers are colder than those of the other places named. The second city selected, Rasht, has such a temperate and humid climate that it rains almost every day of the year there. The Caspian Sea border experiences this climate, which results in consistent annual rainfall. As a result, this city has warm winters and hot, muggy summers without a dry season. Table 2 shows the physical and climatic features of the chosen cities in the following.

Fig. 2. Map of Iran based on the division of Pourheidari et al [55].

Table 2. Physical and climatic characteristics of selected cities.

Cites	Climatic	latitude (degrees)	longitude (degrees)	height (meters)	HDD	CDD
Bandar Abbas	Warm and humid	27.22	56.37	10	1776	249
Tehran	Warm and dry	35.41	51.19	1190	1810	824
Rasht	Moderate and humid	37.33	49.61	-12.2	1818	268
Shahrekord	Cold	32.29	50.84	2049.2	3226	327

Figure 3 depicts the average temperature graph of several Iranian cities based on meteorological data. It indicates that, generally speaking, all Iranian cities had their greatest temperature increases during June, July, and August. Thus, the months of January and February saw the lowest average temperature fall. Because of their closeness to the desert, southern cities experience extremely hot summers, but their winters are generally milder than those of other parts of the nation. Consequently, when compared to other Iranian cities, Bandar Abbas has had the greatest temperature increase. Temperatures in this city have occasionally reached as high as 10 degrees Celsius in January and as high as 54 degrees Celsius in June. In the summer, Bandar Abbas sees relatively little temperature change between day and night due to high humidity levels; however, throughout the winter, there is a higher temperature difference between day and night. Shahrekord, on the other hand, has lower humidity than other Iranian cities since it is situated farther from the sea and at a higher height than other towns. It has frigid winters and scorching summers with significant day-to-night temperature variations as a result. Shahrekord has a very large temperature differential, with the air reaching 42 degrees Celsius during the day and 4 degrees Celsius at night. Shahrekord has frigid winters during the colder months of the year; on occasion, the temperature in January falls as low as minus 18. But this season's night and day temperature differences are less pronounced because of the higher humidity than in the summer. The city of Rasht has significant levels of humidity and rainfall because of its closeness to the Caspian Sea. This city's climate is steady and mild because of the prevalence of humidity, which has reduced the variation in temperature between day and night. Because of its vicinity to the Alborz Mountain range and Damavand peak, Tehran experiences chilly winters. However, this same proximity has also contributed to the city's air's correct humidity, which maintains a stable temperature. The phenomena of temperature inversion and increased pollution in this city are caused by the temperature stability at the start of the winter season.

3.2. Characteristics of the studied building and envelope

In this study, a real residential building is modeled in the software. This building consists of six floors, the ground floor of which is the parking lot, and the top five floors have the same plans as shown in Fig. 4.

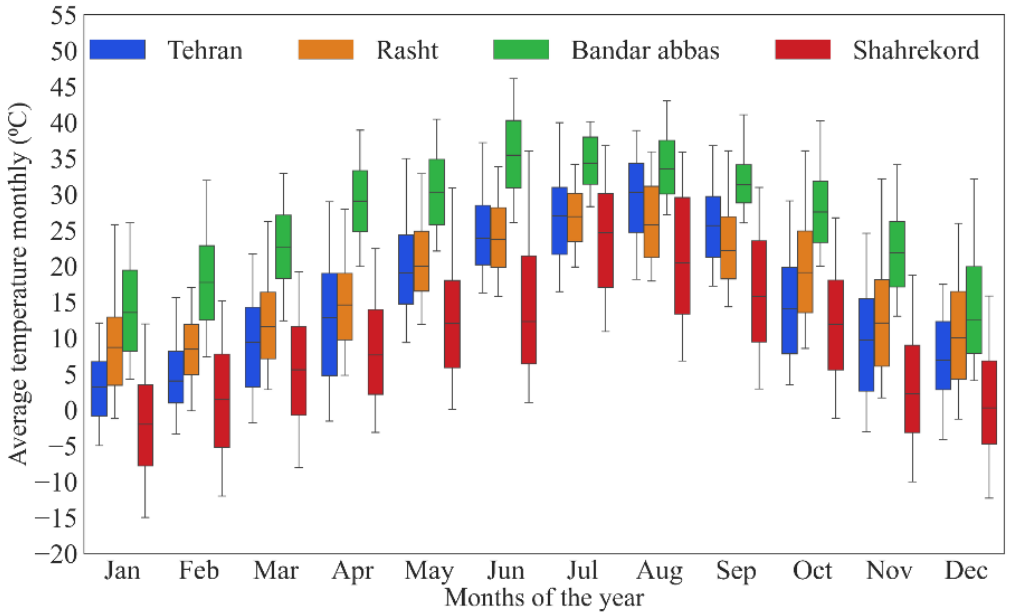

Fig. 3. Temperature chart of different cities of Iran every month.

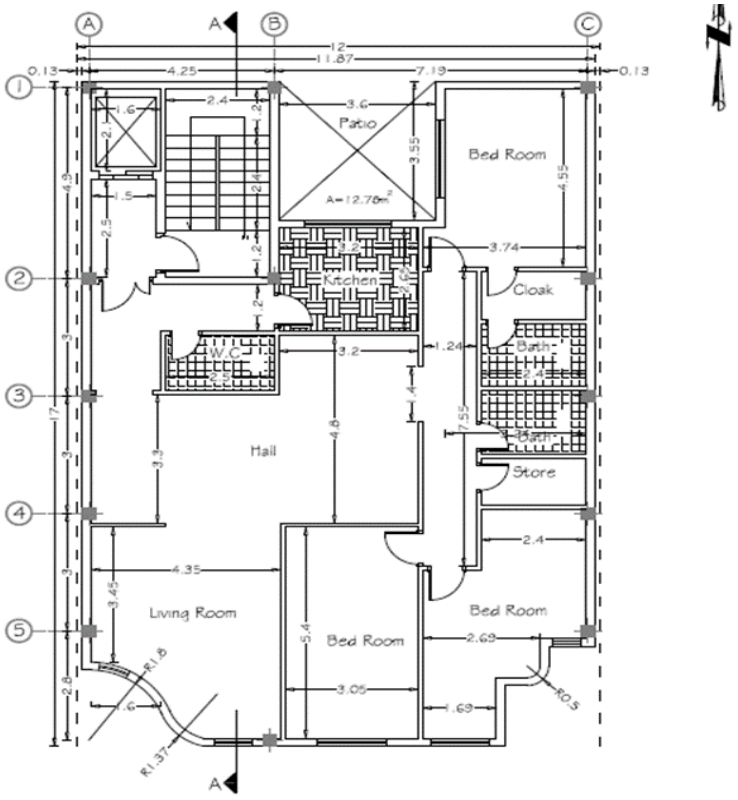

Fig. 4. Executive plan of the building.

Each floor of the residence includes three bedrooms, two bathrooms, a toilet, a kitchen, a hall and reception, a storage room, and a patio. The shape of the building, the characteristics, and the area of the spaces are shown in Fig. 5 and also in Table 3.

Three building coverage classes have been proposed, as per issue 19 of Iran's National Building Laws and Regulations [56]. Cities with varying climates are categorized into these three groups based on their energy level. These categories, which are based on the energy needs of the building envelope, are divided into three categories: high, medium, and low energy levels. To ensure that the value of the thermal resistance coefficient (R-V) is respected, a reference value has been provided for each classification. Table 4 indicates the recommended value of the thermal resistance coefficient for the walls by this topic. Additionally, values have been suggested for transparent walls, or windows, by this issue; these values are included in Table 5.

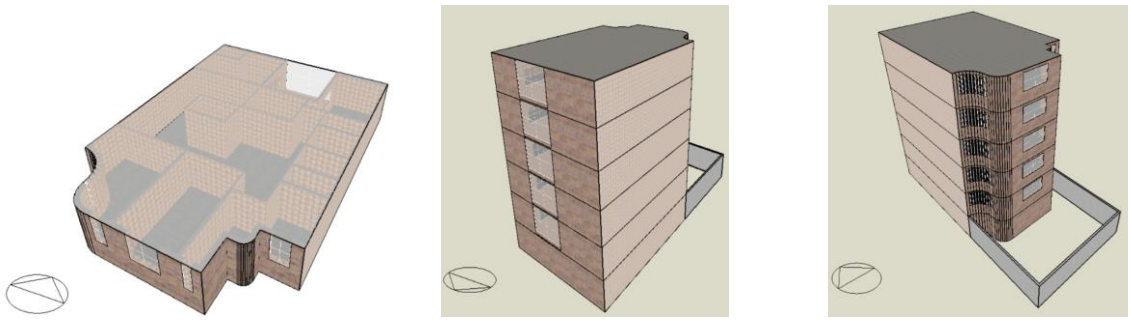

Fig. 5. A view of the investigated building.

Table 3. Physical characteristics of building spaces.

Space	Floor area (m^2)
Bedroom 1	16.47
Bedroom 2	13.436
Bedroom 3	16.34
Kitchen	8.608
Living room	21.5
Hall and reception	40.167
Bathroom 1	4.55
Bathroom 2	4.55
Wc	4.72
Store	2.86
Entrance floors and stairs	20.83
Parking	178.02
Patio	12.78

Table 4. the amount of insulation thickness suitable for covering the building [56].

Cites	External Wall $\left(\frac{m^2.K}{W}\right)$	Adjacent wall of un-conditioned space $\left(\frac{m^2.K}{W}\right)$	Roof $\left(\frac{m^2.K}{W}\right)$	Floor adjacent to air $\left(\frac{m^2.K}{W}\right)$	Floor adjacent to soil $\left(\frac{m^2.K}{W}\right)$
Tehran	1.5	0.8	2.4	2.5	0.7
Shahrekord	1.5	0.8	2.4	2.5	0.7
Rasht	1.2	0.7	2	2	0.5
Bandar Abbas	2.3	1	3.3	3.5	0.7

Table 5. physical and optical characteristics of transparent windows [56].

Cites	Direction	U-Value $\left(\frac{W}{m^2.K}\right)$	Normal solar factor	Normal visible transmittance
Tehran, Shahrekord,	South	3.1	0.5	0.55
	North	3.1	0.5	0.55
	East/West	3.1	0.36	0.504
Rasht	South	3.1	0.5	0.55
	North	3.1	0.5	0.55
	East/West	3.1	0.4	0.56
Bandar Abbas	South	3.1	0.4	0.48
	North	3.1	0.5	0.5
	East/West	3.1	0.35	0.49

3.3. Internal loads, schedules and HVAC

In this study, inside-building illumination requirements have been established by Topic 13 of Iran's National Building Regulations [57]. Values based on the type of building are proposed for the amount of lighting inside the buildings, which have been used for lighting in the interior spaces of the residential building considered in this study, as shown in Fig. 6 and Table 6, in the second appendix of topic 13 of Iran's National Building Law and Regulations [57].

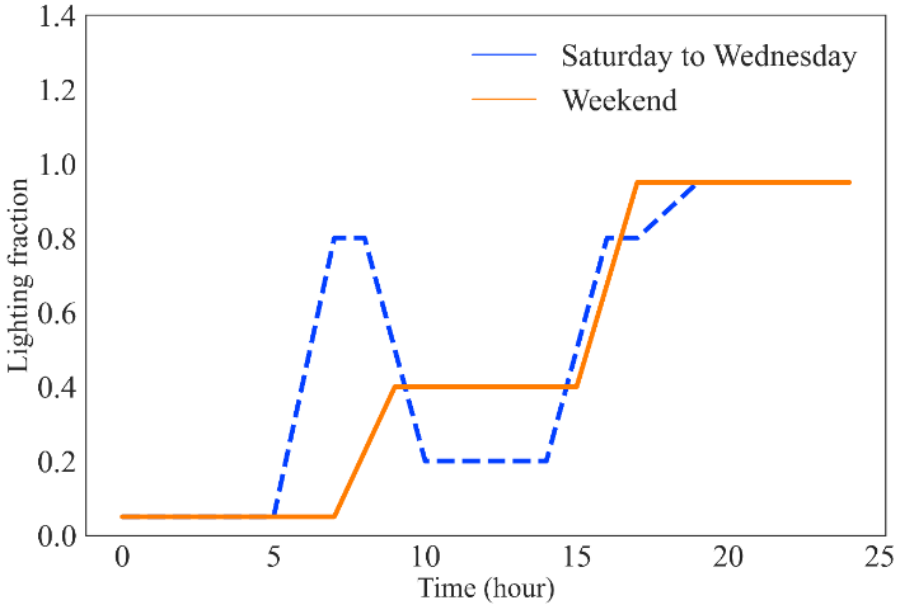

Fig. 6. Amount and working hours of building lighting.

Table 6. Luxury amount consumed in different spaces of the building [57].

Space	The required amount of light (lux)
Bedroom	100
Kitchen	200
Store	100
Living room	200
Hall and reception	200
Bathroom and toilet	100
Patio	100
Staircase and entrance	100
Parking	100

Also, the amount of electricity consumed by all types of electrical equipment in residential buildings is shown in Table 7.

4 people are living on each floor of this building, whose schedule is shown in Fig. 7, based on topic 19 of the National Building Regulations of Iran [56].

Initially, the ideal load technique was used to determine the building's heating and cooling loads for each intended building in each city. The temperature of the heating and cooling thermostats in all Iranian cities, except Bandar Abbas city, should be 20 degrees Celsius and 28 degrees Celsius, respectively, at all times of the day and night, by issue 19 of Iran's construction laws and national regulations [56]. However, it is between 20 and 25 degrees Celsius in Bandar Abbas.

The cooling and heating loads of the desired building in the ideal load system for the city of Tehran are 20.019 and 29.840 kilowatts, respectively, with electricity consumption of 22185.67 and 45595.05-kilowatt hours for Rasht city, respectively, and 14.369 and 26.647 kilowatts with electricity consumption of 9253.9253 and 43816.7-kilowatt hours, respectively, for Shahrekord city, 9.2839 and 37.4526 kilowatts and electricity consumption of 2151.44 and 69318.23-kilowatt hours. Finally, for the city of Bandar Abbas, it is 27.102 and 10.233 kilowatts, respectively, with electricity consumption of 154794.84 and 402.31 kilowatt hours. Now, according to the amount of loads calculated in each city, radiator with evaporative cooler, fan coil, PTHP, PTAC, and VRF have been simulated for each, from different companies with cooling and heating capacities. Different systems have been used, and a total of 40 different ACS have been simulated for each city. The technical specifications of the systems used for Tehran can be seen in Tables 8-16.

Table 7. The amount of electricity needed for building electrical appliances.

Electrical equipment	Amount of electricity required (watts)
Laptop	100
fryer	1500
Television	100
Refrigerator	350
washing machine	350
Otto	1800
vacuum cleaner	1000
dishwasher	1200

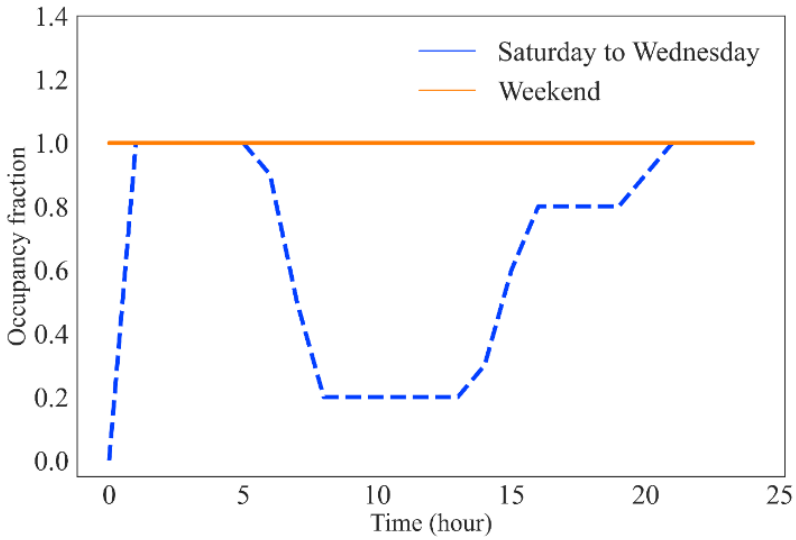

Fig. 7. Attendance schedule of people.

Table 8. Technical specifications of the investigated types of radiators.

Diameter pipe (in)	Heat capacity of each vane (kcal/h)	Material	Weight of each vane (kg)	Model
1	115	aluminum	0.85	Eco 500 radiator [58]
1	156	aluminum	1.4	Butane radiator Elena model [59]
1	157	aluminum	1.4	Il Primo radiator [59]
1	152	aluminum	1.5	Kal 500 radiator [58]
1	135	aluminum	1.46	Maxi radiator [58]
1	126	aluminum	1.35	Thermo radiator [58]
1	154	aluminum	1.4	Vitoria radiator [59]

Table 9. Technical specifications of types of evaporative coolers.

Pad dimensions (cm)	Weight (kg)	Engine power (hp)	Aeration capacity (m^3/hr)	The amount of pump water (lit/min)	Model
90*80	73	1.2	6150	12	Mashhad Davam MD-6500 model [60]
90*100	83	3.4	4900-8350	12	Absal model AC70 [61]

Table 10. Technical specifications of cast iron boilers used in the radiator and fan coil ACS.

Maximum working temperature(°C)	Weight (kg)	Boiler water volume (lit)	Maximum capacity (kW)	Model
90	175	17	36	Cast iron boiler Super 200 Shofajkar [62]
90	147	14	38.7	MI3 model S90-3 [63]

Table 11. Technical specifications of chillers used by fan coils.

EER	Refrigerant type	Refrigeration capacity (ton)	Power (kW)	Refrigerant weight (kg)	Capacity (kW)	Model
3	R410	8.5	10	7	30	Media air-cooled chiller model MGB-D30W/R [64]

Table 12. Technical specifications of all types of fan coils.

Weight (kg)	Heating capacity (kW)	Cooling capacity(kW)	Maximum aeration capacity (CFM)	Model
31	7.22	3.27	400	DT. GC400 DamaTajhiz fan coil [65]
25	6.79	4.01	400	Goldiran built-in ceiling fan coil model GLKT400 [66]
16.3	6.41	3.77	400	Goldiran GLKG-400 one-way Cassette fan coil [67]
25.6	8.7	5.3	400	Built-in ceiling fan coil G-Plus model GFU-LC400G30 [68]
25	6.79	4.19	400	Media built-in ceiling fan coil with three-row MKT3-400 coil [69]
26	7.21	3.27	400	Media ground fan coil model MKF-400 [70]
27	6.79	3.75	400	MKC-400 one-way case Cassette media fan coil [71]
30	6.38	1.83	200	Saran SRFCSE-200 Ground Fan Coil [72]
23.7	8.1	5.4	600	Green built-in ceiling fan coil model GDF600P1 [73]

Table 13. Technical characteristics of PTHP systems.

Refrigerant type	Power (W)	EER	COP	Heating capacity (Btu)	Cooling capacity (Btu)	Model
R410	835	3.03	3.41	10400	8670	9000 IRAN RADIATOR [74]
R410	748	3.34	4.25	10000	9000	9000 TRUST [75]
R410	845	3.41	4.2	9400	9000	9000 HOMAX [76]
R410	790	3.05	3.5	9554	9000	9000 Gary [77]
R410	715	3.72	4.08	10000	9000	9000 GREEN [78]
R410	750	3.43	3.73	10000	9000	HYUNDAI 9000 model 0930W [79]
R410	845	3.34	3.7	9600	9000	HYUNDAI 9000 model 0932WT1 [80]
R410	2000	3.32	3.65	25000	24000	24000 GREEN [81]
R410	1900	3.22	5.27	24500	24000	24000 General Gold [82]
R410	2200	3.21	3.61	24000	9000	PAKSHOMA model 24CH [83]
R410	2280	3.02	3.41	28150	24500	24000 KAZUKI [84]
R22	2800	2.44	3.5	30000	12000	Cold 24000 PAKSHOMA [85]

Table 14. Technical specifications of PTAC systems.

Refrigerant type	EER	COP	Heating capacity (Btu)	Cooling capacity (Btu)	Model
R410	12.8	3.8	8100	9000	Direct supply [86]
R410	12.1	3.5	8000	9000	LG [87]

Table 15. Technical characteristics of external units of VRF systems.

Refrigerant type	Power (W)	EER	COP	Heating capacity (Btu)	Cooling capacity (Btu)	Model
R410	5210-5270	4.3	4.33	85000	76000	HISENSE [88]
R410	5900-6800	3.29	4.15	84000	76000	BOYMAN [89]
R410	7900-8400	3.1	3.61	98000	90000	GREEN [90]

Table 16. Technical characteristics of external units of VRF systems.

Maximum aeration (m^3/hr)	Power (W)	Heating capacity (kW)	Cooling capacity(kW)	Model
1006	72	7.1	6.3	HISENSE [91]
1200	35	8	7.1	BOYMAN [92]
1200	82	8	7.1	GREEN [93]

3.4. Costs

This section explains the calculation technique for each of the three utilities—water, gas, and electricity—and how each is computed based on the tariffs supplied by the relevant firms. The CIACS will then be mentioned.

3.4.1. The cost of gas bills

According to the announcement of Iran's Ministry of Gas [94], gas cost calculation is divided into two parts. The first part, which is the same for all cities, belongs to the warm season of the year.

However, for the cold season of the year, it is divided into five zones. The cities of Tehran, Shahrekord, Bandar Abbas, and Rasht are located in regions 3, 2, 5, and 3, respectively. These tariffs can be seen in Table 17.

Table 17. Tariff for gas consumption in the domestic sector for a) Hot months of the year and b) Cold months of the year [94].

(a)

2	3	4	5	6	7	8	9	10	11	12
46-95	96-145	146-195	196-245	246-295	296-345	346-395	396-445	446-495	496-545	More than 545
0.0357	0.0429	0.0471	0.0519	0.57	0.0627	0.069	0.076	0.0835	0.092	0.101

(b)

2	3	4	5	6	7	8	9	10	11	12
301-400	401-500	501-600	601-700	701-800	801-900	901-1000	1001-1100	1101-1200	1201-1300	More than 1300
251-350	351-450	451-550	551-650	651-750	751-850	851-950	951-1050	1050-1150	1151-1250	More than 1250
201-300	301-400	401-500	501-600	601-700	701-800	801-900	901-1000	1001-1100	1101-1200	More than 1200
151-250	251-350	351-450	451-550	551-650	651-750	751-850	851-950	951-1050	1051-1150	More than 1150
76-150	151-250	251-350	351-450	451-550	551-650	651-750	751-850	851-950	951-1050	More than 1050
0.01643	0.023	0.0322	0.0451	0.06312	0.0884	0.1237	0.1732	0.2424	0.3394	0.4752

Domain of consume	1
Domain (m^3)	until the 45
Tariff ($)	0.0321

Domain of consum	1
Climate 1	until the 300
Climate 2	until the 250
Climate 3	until the 200
Climate 4	until the 150
Climate 5	until the 75
Tariff ($)	0.00985

3.4.2 .The cost of water bills

In the water sector, according to the announced tariff of the Water Department [95], we have a fixed price for decimalization, which is multiplied by the coefficient of each city to calculate the price of each cubic meter of water consumed in the residential building sector of that city. The basis of the work according to the tariff of the Tithe Water Administration is announced based on the amount of water consumption of the buildings, which can be seen in Table 18. These numbers are the base price in each consumption decile, which is multiplied by the coefficient provided by the water department for each city to obtain the basis for calculating each cubic meter of water consumption in that city. The coefficient of the desired cities for calculation is shown in Table 19. For example, for the city of Tehran, the first consumption decile is calculated according to the Tables 18-19, according to Eq. (1).

$$\begin{aligned}&\text{The cost of each cubic meter of water use}\\&= \text{Tariff for every tenth of consumptic}\\&* \text{The impact factor of each city}\end{aligned} \quad (1)$$

3.4.3. The cost of electricity bills

According to the tariff announced by the Ministry of Energy of Iran [96], special laws have been adopted for those cities in Iran that have relatively hot weather and relatively high humidity in the hot months of the year. For this purpose, for some hot and cold months of the year, it has published separate tables to calculate the amount of electricity consumption, and these published tables have been divided into four tropical regions. For example, for the city of Rasht, the amount of electricity consumption by household customers is calculated based on the table published in the tropical region of four, only for 3.5 months of the year (June 1st to September 15th). The daily electricity consumption of household subscribers is divided into three categories: low load (from 23:00 to 7:00 a.m. a day), medium load (from 7:00 a.m. to 7:00 p.m. a day), and peak load (from 7:00 p.m. to 11:00 p.m. a day) will be the peak load of electricity consumption as well as its low load calculated in the form of a fixed rate (peak load 794 rials and low load 397 rials) as well as the amount of intermediate loads according to Tables 20-21. How to calculate the cost of electricity consumption purchased by household subscribers from the Ministry of Energy is calculated according to Eq. (2). According to the type of tariff announced by the Ministry of Energy, the relevant settings for the electricity sector have been made in the Energy Plus software, and all electrical appliances such as the ACS itself, pumps, lighting, etc. have been calculated inside it.

$$\begin{aligned}&\text{The cost of electricity consumption}\\&= Medium\ \ peak\ \ cost\\&- off\ \ peak\ \ cost\\&+ High\ \ peak\ \ cost\end{aligned} \quad (2)$$

Table 18. Tariff for water consumption [95].

Price relative to surplus (dollars per cubic meter)	Consumption floors (cubic meters per month)	Row
0.0672	0-5	1
0.1007	5-10	2
0.134	10-15	3
0.1755	Up to 1.5 times the consumption pattern	4
0.5*free price	1.5 to 2 times the consumption pattern	5

0.75*free price	2 to 3 times the consumption pattern	6
3*free price	3 to 4 times the consumption pattern	7
5*free price	More than 4 times the consumption pattern	8

Table 19. Water cost impact factor [95].

City	Coefficient
Tehran	1.49
Rasht	1.27
Shahrekord	1.29
Bandar Abbas	1.4

Table 20. Electricity cost at a normal rate [96].

Average monthly energy consumption (per kWh)	Base price per kilowatt hour (dollars)
0-100	0.019
100-200	0.022
200-300	0.0472
300-400	0.085
400-500	0.097
500-600	0.123
More than 600	0.135

Table 21. The cost of electricity at the rate of the tropical zone four [96].

Average monthly energy consumption (per kWh)	Base price per kilowatt hour (dollars)
0-100	0.015
100-200	0.018
200-300	0.0315
300-400	0.05
400-500	0.0724
500-600	0.0944
More than 600	0.1133

3.4.4. CIACS

In this study, to simulate and optimize the ACS in the desired building, by combining heating and cooling ACS and also using several samples of different models from companies producing a specific ACS. Such as fan coils, radiators, etc. have been used, and a total of 40 different ACS have been examined in this study. The name and total cost of purchase, installation and, commissioning of each of these ACS along with the names of their manufacturing companies can be seen in Table 22. The installation and operation of each of these reviewed ACS are added to the initial cost of their purchase, hence the installation and operation cost of each ACS is different from the other, for example, for evaporative coolers, the purchase cost and installation of the evaporative cooler itself along with the cost of constructing and installing the cooler channel is added to its total costs.

3.5. Determination of decision-maker variables and objective functions

In the study, the design variables are the SCIL, WCIL, different ACS, HTT, and CTT. Our target functions in this research are CIACS, ACB, and PPD. The required design variables produced by the JEPlus toolbox can be seen in Table (23).

Table 22. CIACS.

ACS	Cost (dollars)	ACS	Cost (dollars)	ACS	Cost (dollars)	ACS	Cost (dollars)
Hisense VRF system	82348.36429	Media fan coil	70459.85714	Hyundai PTHP	75357.14286	Mashhad davam evaporative cooler and Maxi radiator	58075.97619
Boyman VRF system	72783.08571	Media fan coil	71251.52381	Green PTHP	40327.38095	Mashhad davam evaporative cooler and Vitoria radiator	57669.72857

Table 22. CIACS

ACS	Cost (dollars)	ACS	Cost (dollars)	ACS	Cost (dollars)	ACS	Cost (dollars)
Green VRF system	84636.78571	Media fan coil	83691.90476	General Gold PTHP	75357.14286	Mashhad davam evaporative cooler and Elena radiator	57385.61905
LG PTAC system	141941.0714	Saran fan coil	70352.61905	Pakshoma PTHP	40308.33333	Absal evaporative cooler and Kal radiator	59377.57214
Direct Supply PTAC system	178569.6429	Iran radiator PTHP	82142.85714	Kazuki PTHP	35928.57143	Absal evaporative cooler and Eco radiator	56483.43405
Green fan coil	72293.19048	PTHP Trust	150000	Pakshoma PTHP	56434.52381	Absal evaporative cooler and Thermo radiator	60969.66667
Dama Tajhiz fan coil	64875.33333	HOMA X PTHP	149628.5714	Mashhad davam evaporative cooler and Kal radiator	59187.09595	Absal evaporative cooler and promo radiator	57710.14286
Goldiran fan coil	65322.95238	Gray PTHP	141285.7143	Mashhad davam evaporative cooler and Eco radiator	56102.48167	Absal evaporative cooler and Maxi radiator	58266.45238
Goldiran fan coil	83099.14286	Green PTHP	170292.8571	Mashhad davam evaporative cooler and Thermo radiator	60779.1948	Absal evaporative cooler and Vitoria radiator	57840.14286
G-Plus fan coil	67674.14286	Hyundai PTHP	142857.1429	Mashhad davam evaporative cooler and promo radiator	57519.66667	Absal evaporative cooler and Elena radiator	57576.09524

Table 23. Decision maker variables.

Design variables	Unit	Type	Range
SCIL	Clo	Continuous	(0,2)
WCIL	Clo	Continuous	(0,2)
HTT	ºC	Continuous	(15,22.5)
CTT	ºC	Continuous	(23,30.5)

Different ACS	kw	Discrete	According to the Tables 7 to 15 ACS

The level of clothing of people in summer and winter is considered as the variable of people in the building, which according to the level of clothing in each season of the year and in each geographical region under investigation, the best performance of the cooling and heating ACS for the PPD of people The interior of the building has been obtained. Adjusting the operating temperature in ACS, both for cooling and for heating, becomes a factor for better PPD of people inside the building. In this way, a specific ACS in Tehran city may have a different operating temperature compared to Bandar Abbas city, so that people feel better PPD in the climate of each city, hence the set temperature in the operating thermostat of the devices. considered variable. Another factor in the investigations is the use of different ACS in each city, which have the best performance of the ACS for heating and cooling in the building space, according to the type of climate and the geographical location of each city under investigation.

4. Results

4.1. Sensitivity analysis

To check the influence of variables of the design decision maker on the required objective functions, a tool called sensitivity analysis should be used in the research. As mentioned in the previous chapters, this analysis determines the influence and participation of the decision-making variables on the specified objective functions according to the type of work process. In this research, Morris's sensitivity analysis has been used about these cases, the results of which can be seen in Table 24.

4.2. Optimization

EnergyPlus software, with all its merits and advantages, easily performs simulation operations by itself. However, due to the complexities of this study and the large number of input variables in this research, a method is needed that can perform optimization with simulation simultaneously. It means that the software can call the initial data from the simulation software (i.e. Energy Plus) and then produce its initial results. It examines each input in the range of their changes and for this purpose selects the optimal points according to the specified limits and determined objective functions. Since the main goal is to maintain the PPD of the people inside the building while minimizing CIACS and also reducing the cost of energy consumption, we do not accept the single-objective optimization approach, and the answers are Beam curves are provided by simultaneously determining all three specific objective functions.

Before performing the simulation, it is necessary to determine the initial values of the objective functions. For this purpose, the total initial cost of water, electricity, and gas consumption of the building for all selected cities is shown in Table 25.

Table 24. Sensitivity analysis of Morris for Tehran.

Inputs (decision maker variables)	PPD		ACB (dollars)		CIACS (dollars)	
	μ	σ	μ	σ	μ	σ
Type of ACS	39.97	72.25	85.09	114.7	5117	5868
HTT	10.82	12.19	4.663	6.232	0	0
CTT	13.29	13.16	1.332	3.203	0	0
WCIL	17.13	27.12	0	0	0	0
SCIL	30.21	41.65	0	0	0	0

Table 25. Objective function values before optimization.

Cites	ACB (dollars)	PPD (%)

Tehran	4513.12	22.49
Bandar Abbas	13718	20.9
Shahrekord	3872.48	29.84
Rasht	3437.83	22.79

After specifying the type of decision-making variables in the calculation and its target functions in JEPLUS software, calculations related to optimization must be performed. This software is optimized in a non-dominant way with the help of a genetic algorithm. To optimize the number of generations, the number of populations, the crossover rate, and the mutation rate, 10, 50, 0.8, and 0.02 have been considered for this research. When optimizing in each generation, the software simulates a number of the population and finally selects the optimal points and removes the non-optimal points. This operation continues until it reaches the best and most optimal points, which are called the beam front. In Fig. 8 we can see the optimal points of the beam front for the city of Tehran.

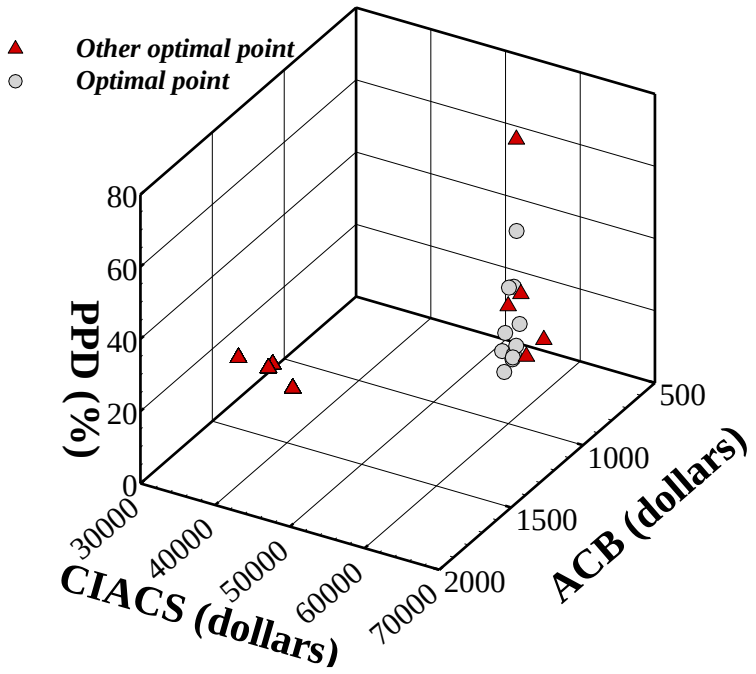

(a)

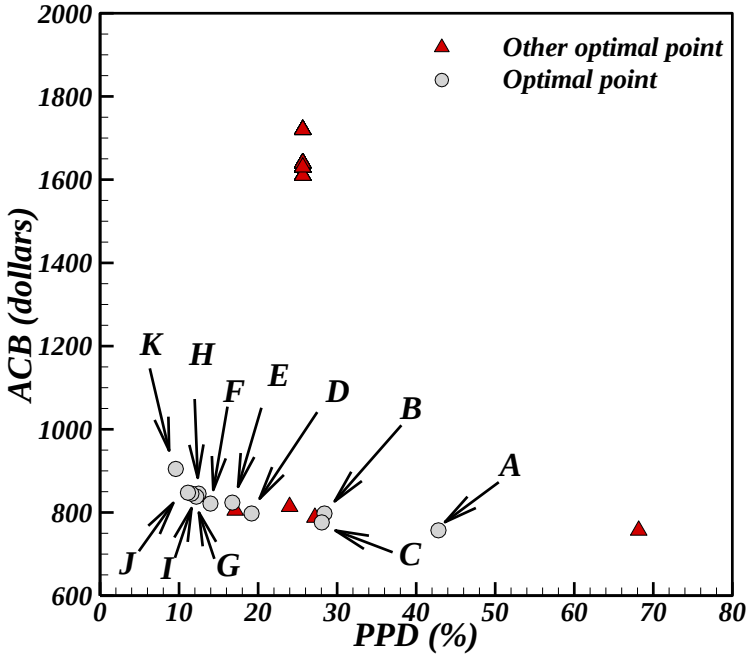
Other optimal point
Optimal point
ACB (dollars)
PPD (%)
2000
1800
1600
1400
1200
1000
800
600
0
10
20
30
40
50
60
70
80
K
H
F
E
D
B
A
J
I
G
C

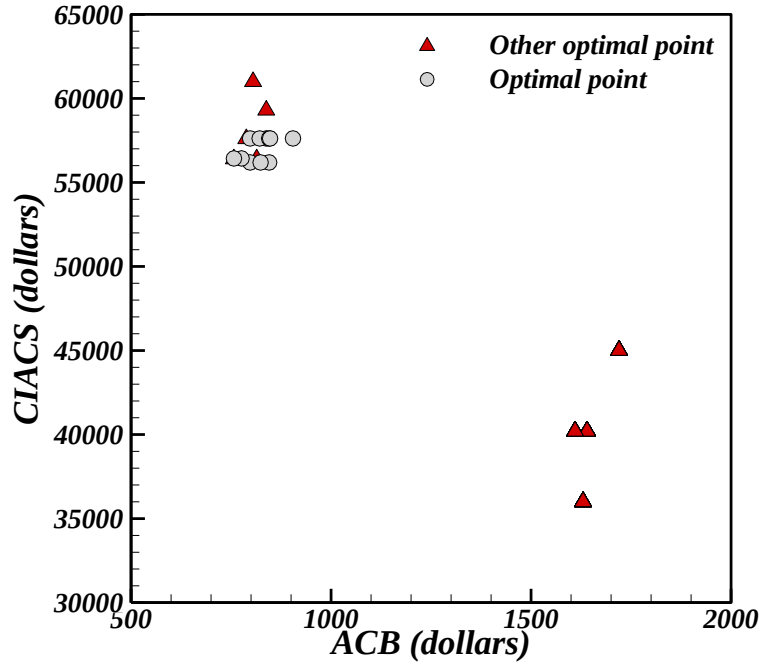
Other optimal point
Optimal point
CIACS (dollars)
ACB (dollars)
65000
60000
55000
50000
45000
40000
35000
30000
500
1000
1500
2000

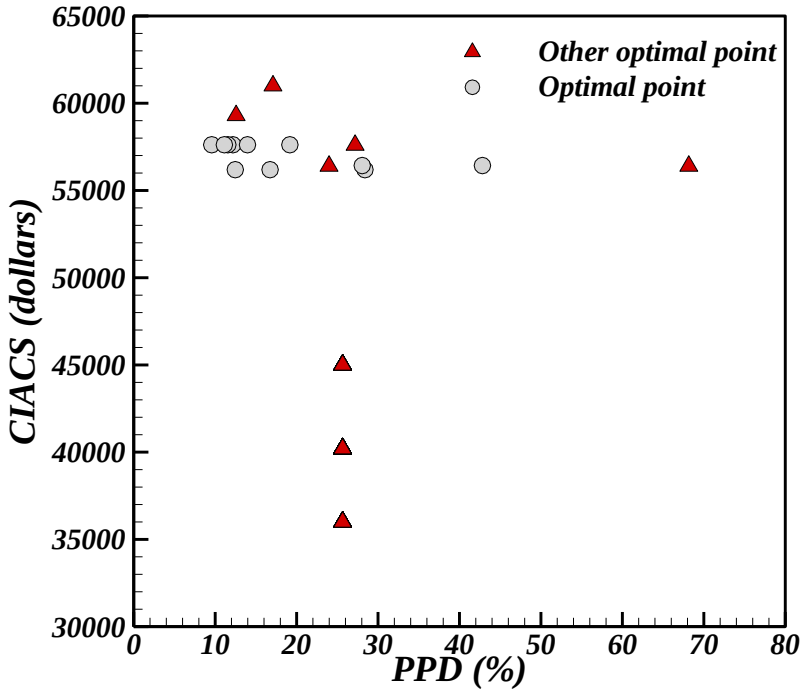

(b)

Fig. 8. Optimal points for the city of Tehran in modes a) 3D plot b) 2D plot

The optimal output points from the JEPLUS+EA software have been imported into the Excel software. To find the best points among the points that the software has given us, we use the WSM weighted sum model method in such a way that we reduce the range of the weighting factor in the weighted sum formula by a distance of 0.1 forward until the best Find the points among all the optimal output points. Finally, 11 points with the characteristics of inputs and outputs were obtained using this method, as shown in Table 26.

Table 26. Optimal points for the city of Tehran.

Coefficient	Type of ACS	HTT (°C)	CTT (°C)	WCIL (Clo)	SCIL (Clo)	PPD	ACB (dollars)	CIACS (dollars)
A	Absal evaporative cooler and Eco radiator	22	29.5	1.9	1.6	42.8	757	56429
B	Mashhad davam evaporative cooler and Eco radiator	15.5	30	1.8	0.5	28.4	798	56190
C	Absal evaporative cooler and Eco radiator	17	26	1.8	0.3	28	776	56429
D	Absal evaporative cooler and Elena radiator	15.5	28	1.9	0.1	19.2	798	57619
E	Mashhad davam evaporative cooler and Eco radiator	17	27.5	1.8	0.5	16.7	824	56190
F	Mashhad davam evaporative cooler and promo radiator	16.5	26.5	1.6	0.5	14	821	57619
G	Absal evaporative cooler and Elena radiator	17.5	25.5	1.8	0.8	12.2	838	57619
H	Mashhad davam evaporative cooler and	17	25	1.5	0.5	12.5	845	56191

	Eco radiator							
I	Mashhad davam evaporative cooler and promo radiator	17.5	25.5	1.7	0.7	11.6	845	57619
J	Mashhad davam evaporative cooler and promo radiator	17.5	25	1.8	0.8	11.1	848	57619
K	Mashhad davam evaporative cooler and Vitoria radiator	19.5	24	1.4	0.7	9.6	905	57619

The lower the value of the PPD number, the better the comfort and well-being of the residents in the building. On the other hand, CIACS for the five-story building in question is relatively high, therefore, according to the above table, point 0.7 has been selected as the most optimal possible mode among the above 11 points. Compared to the other points above, this point has a lower cost for installing and running the ACS. This point has a suitable PPD compared to the initial costs for the installation and operation of the ACS, and it provides suitable PPD for the residents in return for lower paid costs. Also, compared to its neighboring points, point H has a lower ACS installation and commissioning cost, which is a more appropriate number compared to ACB. This cost is $845 for a H point. Also, for points I, G, and F, bills of 845, 838, and 821 dollars are paid for each year, respectively. This small increase is negligible compared to the cost of installation and operation of the ACS, which is approximately $1474 cheaper compared to the points mentioned. The upper and lower points of the table are very different from each other, so that in the lower points there is optimal PPD, but in contrast, CIACS and its ACB are very high. In the upper parts of the table, the costs are as low as possible, but the PPD is extremely inappropriate and does not meet the needs of the people inside the building.

Figures 9-10 show the temperature changes of the cooling thermostat on ACB and PPD. According to Fig. 10, PPD decreases up to 25 degrees Celsius and increases from then on. On the other hand, according to Fig. 9, ACB is the lowest in the temperature range of 24 to 27 degrees Celsius. Therefore, according to the Figures 9-10 as well as the Table 26, the best CTT is 25 degrees Celsius.

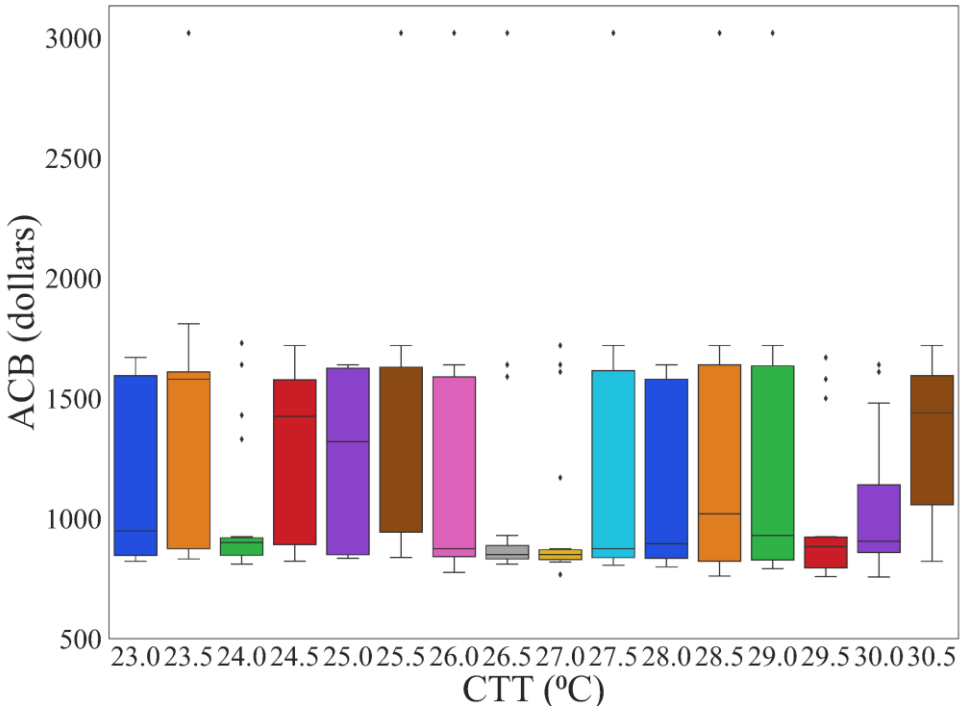

Fig. 9. CTT changes on ACB.

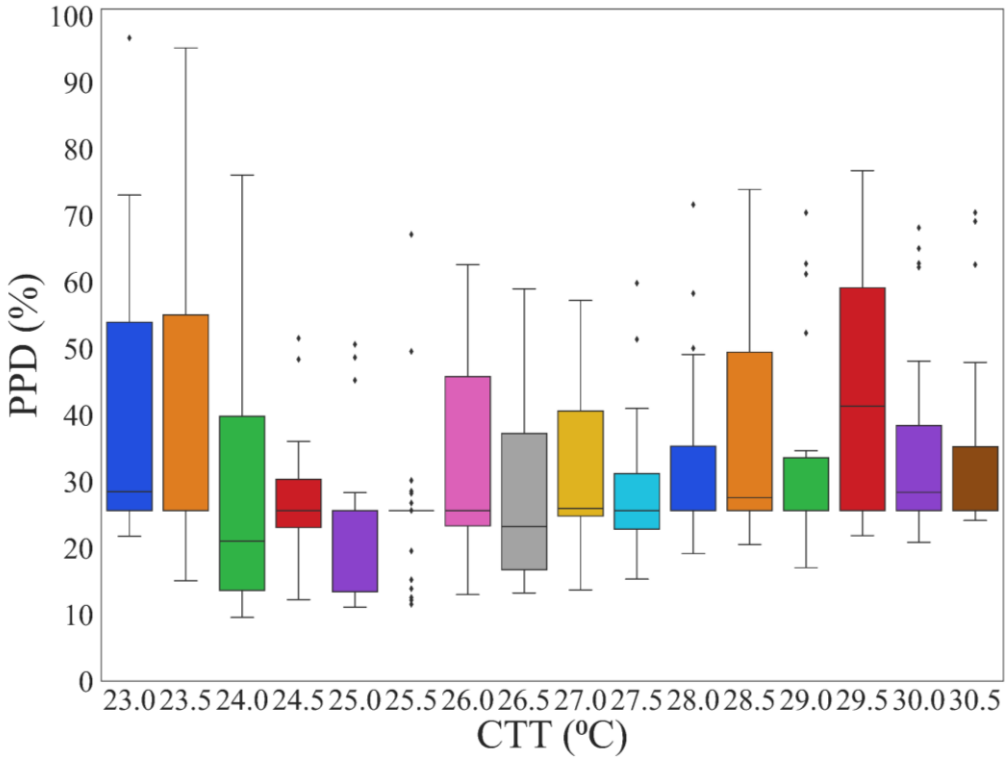

Fig. 10. CTT changes on PPD.

Figures 11-12 show the temperature changes of the heating thermostat on ACB and PPD. According to Fig. 12, PPD decreases up to 17.5 degrees Celsius and increases from then on. On the other hand, according to Figure (11), ACB is the lowest in the temperature range of 15 to 17 degrees Celsius. Therefore, according to the Figs. 11-12 as well as the Table 26, the best HTT is 17 degrees Celsius.

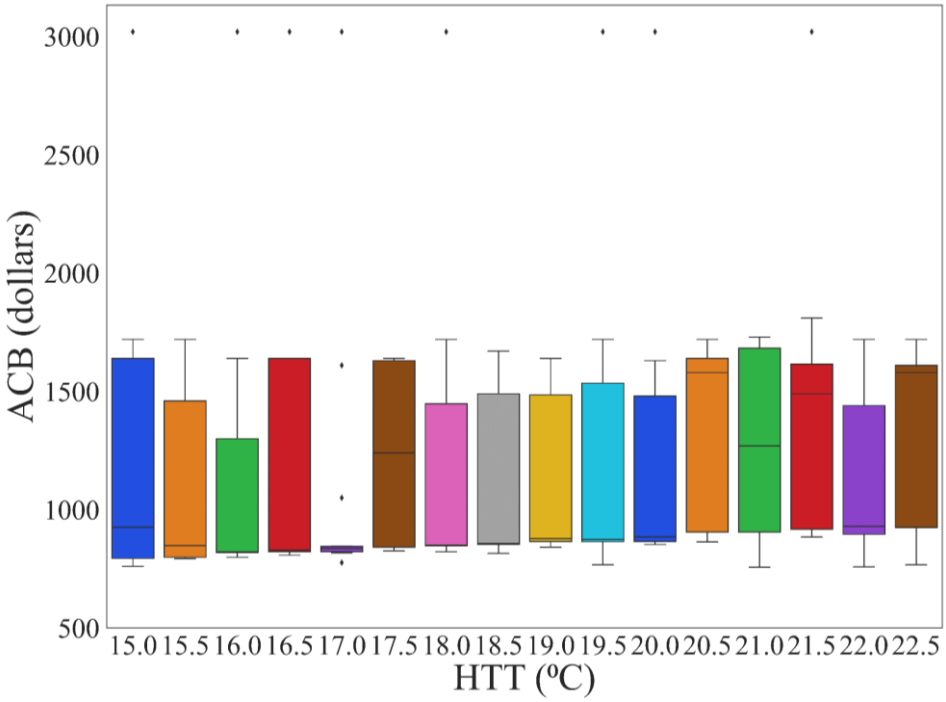

Fig. 11. HTT changes on ACB.

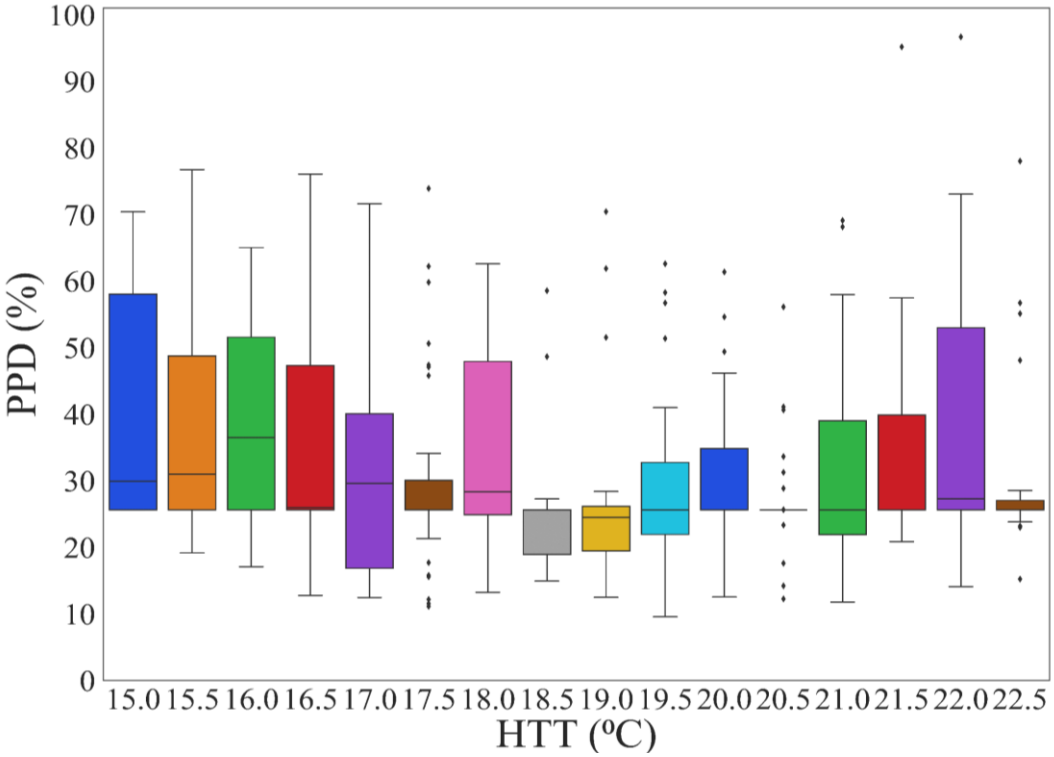

Fig. 12. HTT changes on PPD.

Figures 13-14 show the changes in WCIL and SCIL on PPD. According to Fig. 13, the PPD decreases up to 1, and from then on it is almost fixed. On the other hand, according to Figure 14, it decreases up to the range of 0.5 and remains constant from then on. Therefore, according to Fig. 13-14 as well as Table 26, the best level of winter and summer clothing is 1.5 and 0.5 respectively.

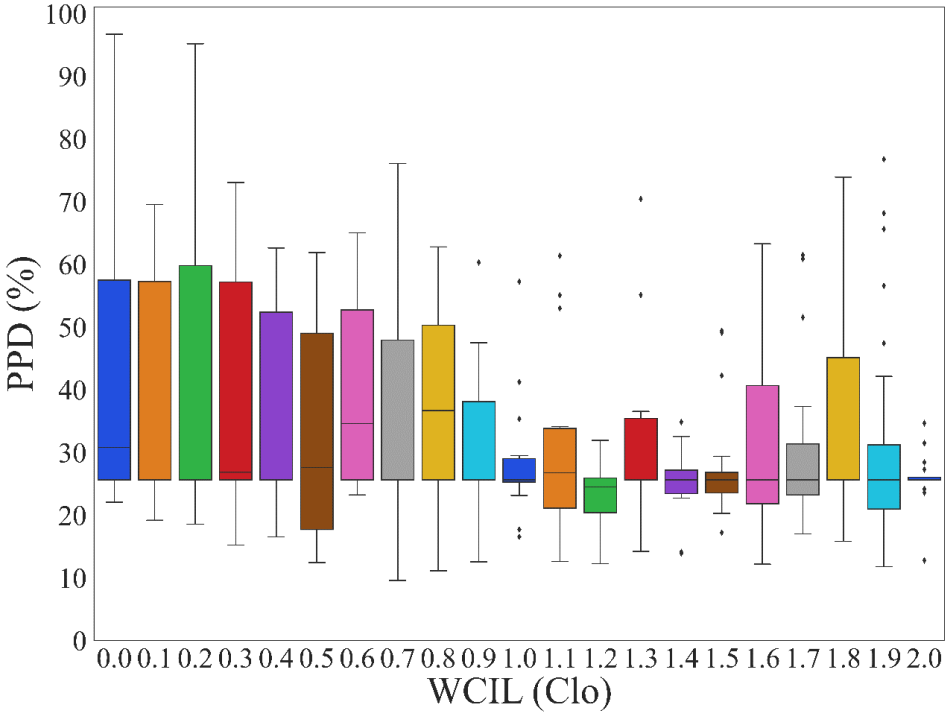

Fig. 13. WCIL changes on PPD.

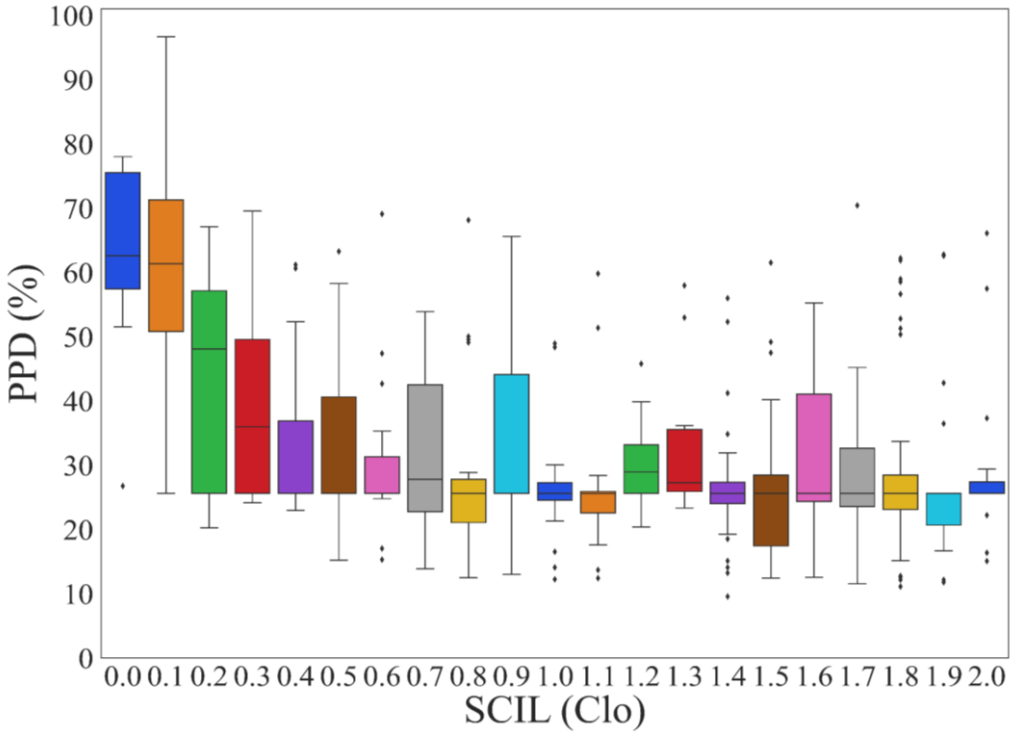

Fig. 14. SCIL changes on PPD.

All the above steps have been carried out for the cities of Shahrekord, Bandar Abbas, and Rasht. In total, the best optimal points for all four cities are shown in Fig. 15 among the exit points of each city, as in the above method, one point was selected as the most optimal point for the four investigated cities, which in Table 27 is shown.

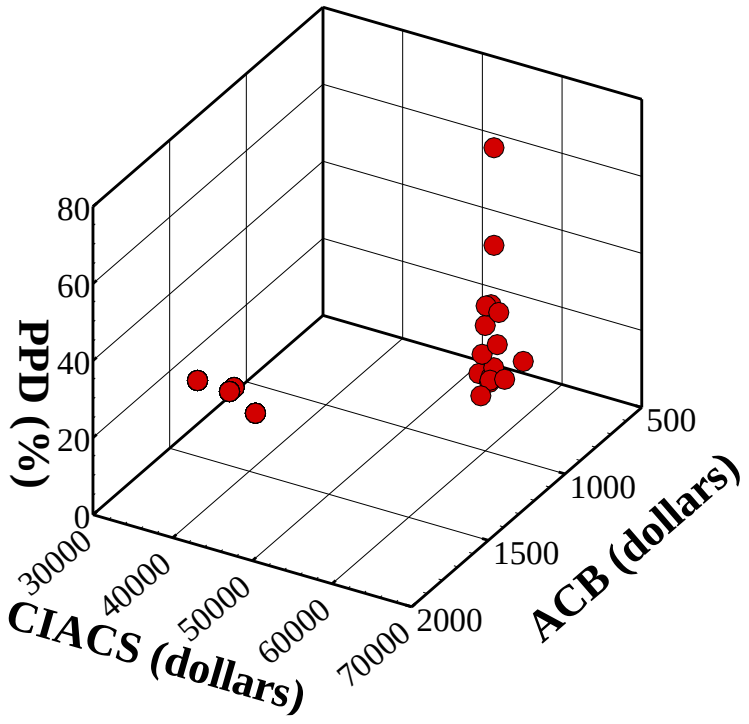

(a)

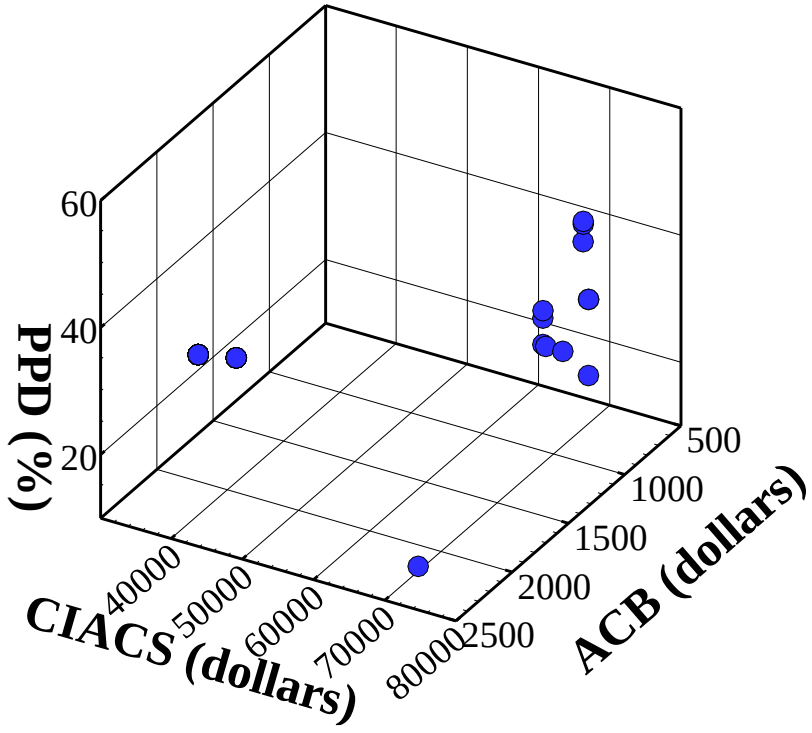
PPD (%)
60
40
20
CIACS (dollars)
40000
50000
60000
70000
80000
ACB (dollars)
500
1000
1500
2000
2500

(b)

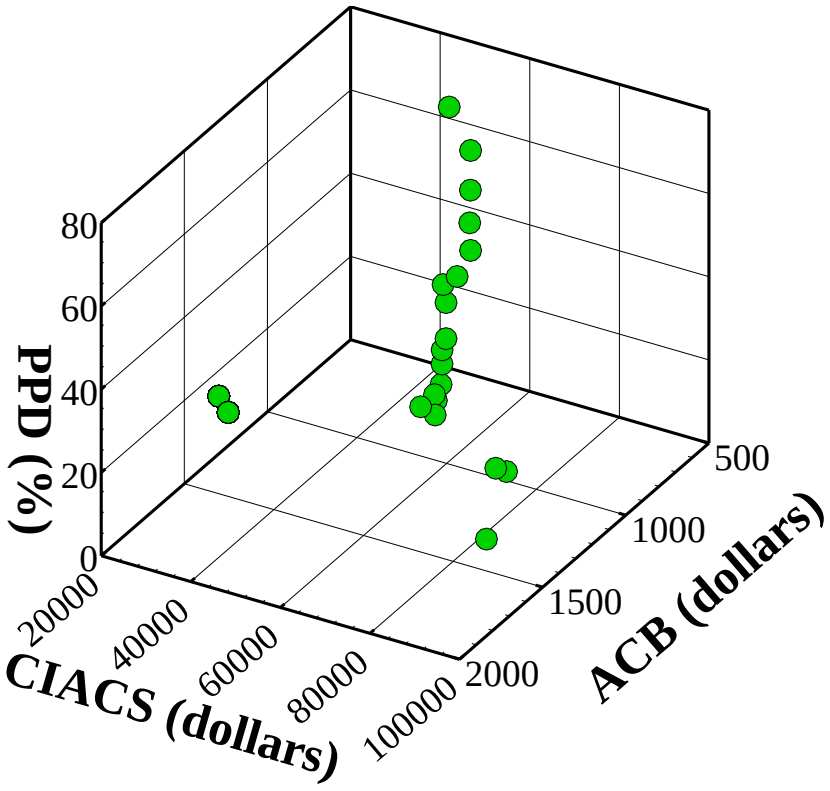
PPD (%)
80
60
40
20
0
CIACS (dollars)
20000
40000
60000
80000
100000
ACB (dollars)
500
1000
1500
2000

(c)

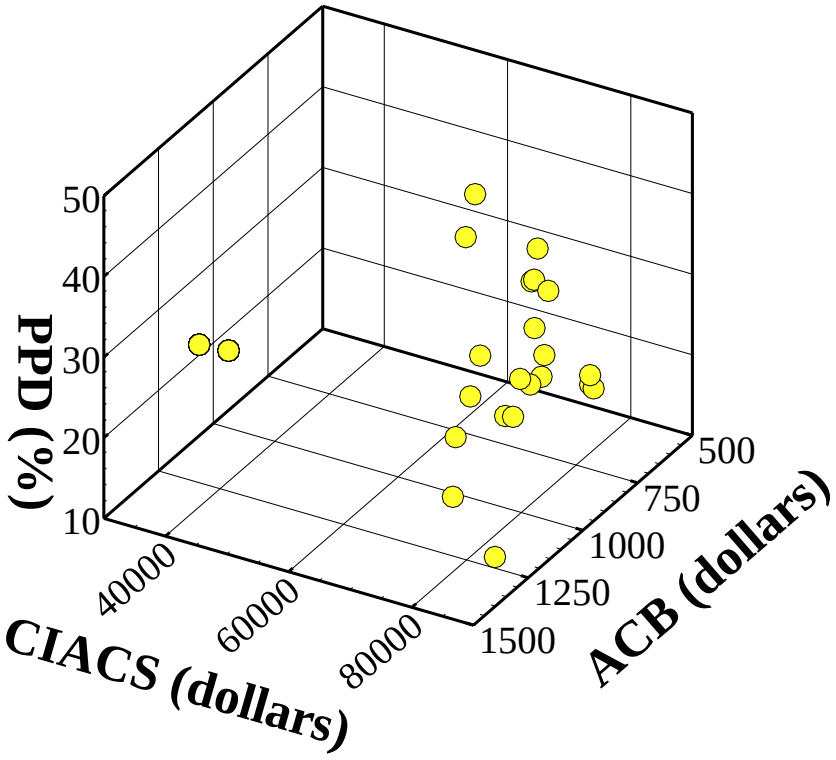

(d)

Fig. 15. Optimum points of Parto front for cities a) Tehran b) Bandar Abbas c) Shahrekord d) Rasht.

It can be seen in Table 27, according to the type of climate in Tehran and Shahrekord cities, the use of a combined system of evaporative cooler and radiator is the best performance against the costs paid for the installation and commissioning of the system and also It has the cost of paying bills. In contrast to the cities of Rasht and Bandar Abbas, due to the high humidity in the air of these two cities, it is very inappropriate to use an evaporative cooler system and this system is not able to cool the air with high humidity. In these two cities, refrigeration ACS should be used to reduce the air humidity to perform heating and cooling in the best possible way. After the optimizations, among these types of systems, the use of the VRF ACS due to its excellent performance and lower electricity consumption than other refrigeration systems, as well as its lower installation and commissioning costs, for these two cities are more suitable.

Table 28 shows the improvement values of the objective functions after optimization. ACB decreased between 63.64% and 82.66% and also PPD improved between 31.1% and 56.3%.

In the following and after the optimizations done for each city, to validate the results obtained in this study, the psychrometric chart can be used. In the psychrometric chart, with the help of the table displayed next to the chart, the separation percentage for the use of different ACS is stated. As can be seen in Fig. 16, for the city of Tehran, the best mode is to use an evaporative cooler for cooling, and for heating, use heating with humidity (such as using a radiator system). As can be seen in Table 27, after optimization, the same type of ACS has been selected for Tehran.

For Shahrekord, based on the psychrometric chart, the best ACS for cooling is to use an evaporative cooler, and the best ACS for heating is to use a combined heating system. It suggests humidity (such as using a radiator system) without reducing the amount of air humidity, which can be seen in Fig. 17. As can be seen in Table 27, after optimization, the ACS of the evaporative cooler with a radiator has been selected for cooling and heating in Shahrekord.

Cooling in the city of Bandar Abbas is of great importance due to the hot and humid climate and the location of this city next to the Southern Dead Sea of Iran. Therefore, the

suggestion of the psychrometric chart is to use the cooling ACS with dehumidification in this city, which can be seen in Fig. 18 and Table 27. The VRF ACS is chosen to optimize energy consumption while maintaining the PPD of the people inside the building. This ACS cools and heats the air with the help of a humidification process with its internal refrigerant gas.

Table 27. Optimal points for the whole city.

Cites	Type of ACS	HTT (°C)	CTT (°C)	WCIL (Clo)	SCIL (Clo)	PPD	ACB (dollars)	CIACS (dollars)
Tehran	Mashhad davam evaporative cooler and Eco radiator	17	25	1.5	0.5	12.5	845	56102
Shahrekord	Absal evaporative cooler and Eco radiator	16	26.5	1.6	1.4	13.04	883	56483
Rasht	Green VRF system	18	23.5	1.6	1.9	11.37	1250	84637
Bandar Abbas	Boyman VRF system	18	25	0.2	1.2	14.4	2379	72783

Table 28. Improvement values of objective functions after optimization.

Cites	Reduction of ACB (%)	Improvement of PPD (%)
Tehran	81.3	44.42
Bandar Abbas	82.66	31.1
Shahrekord	77.2	56.3
Rasht	63.64	50.1

Finally, due to its location in the north of Iran and next to the Caspian Sea, Rasht has a mild and humid climate with a relatively small temperature difference between night and day. Therefore, for the city of Rasht, a dehumidifier ACS is recommended for heating and cooling in this city. The reason for the low percentages displayed in the psychrometric chart is due to the small difference between night and day temperatures and the unstable air temperature of Rasht city, which causes the high humidity of the air to reduce the PPD of people. As can be seen in Table 27 and Fig. 19, VRF ACS is used in this city, which reduces air humidity for use during heating and cooling, and it performs well in this climate.

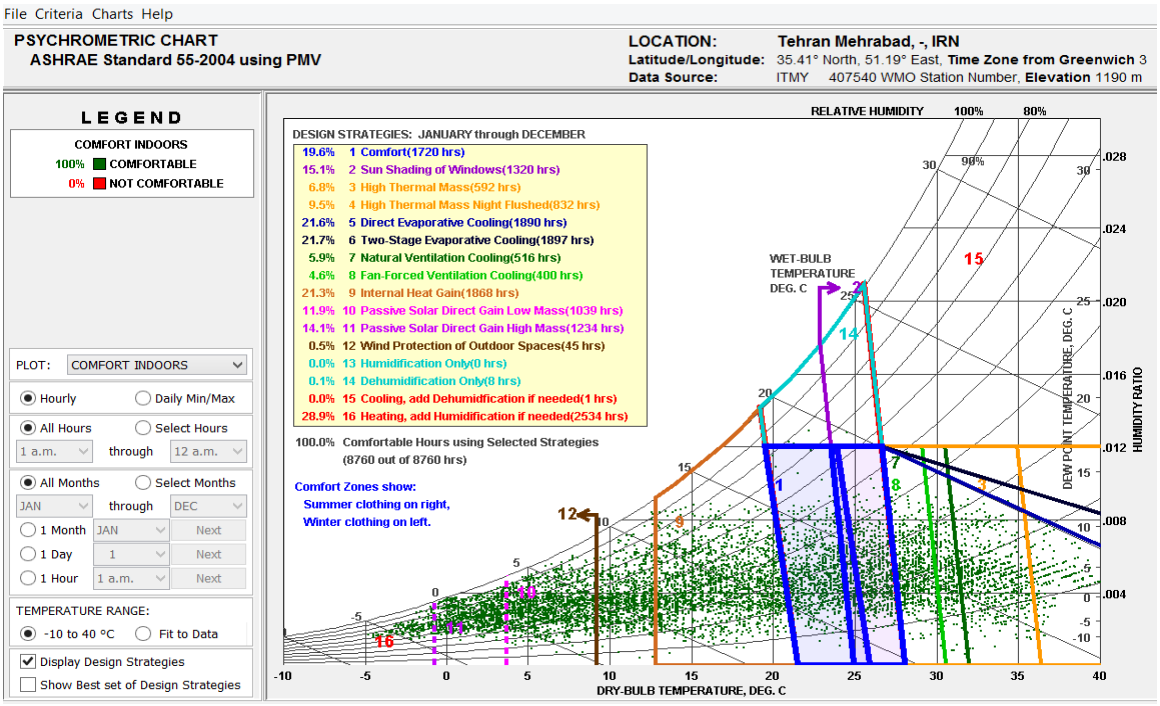

Fig. 16. The type of ACS proposed for Tehran city by the psychrometric chart.

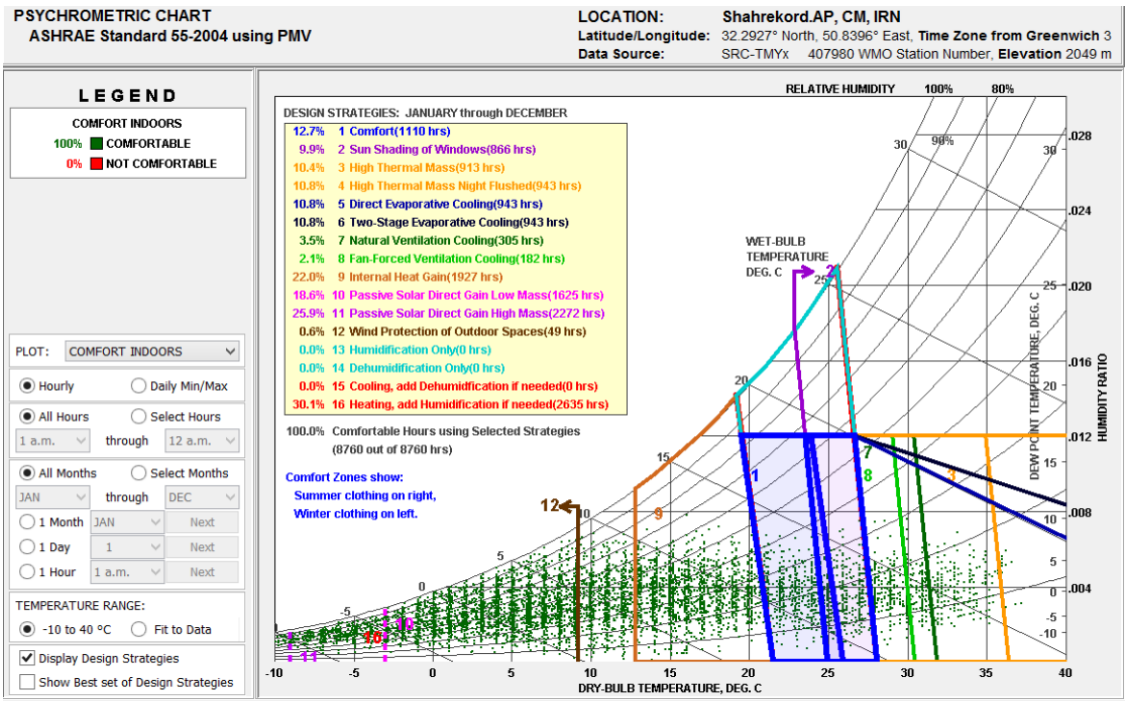

Fig. 17. The type of ACS proposed for Shahrekord city by the psychrometric chart.

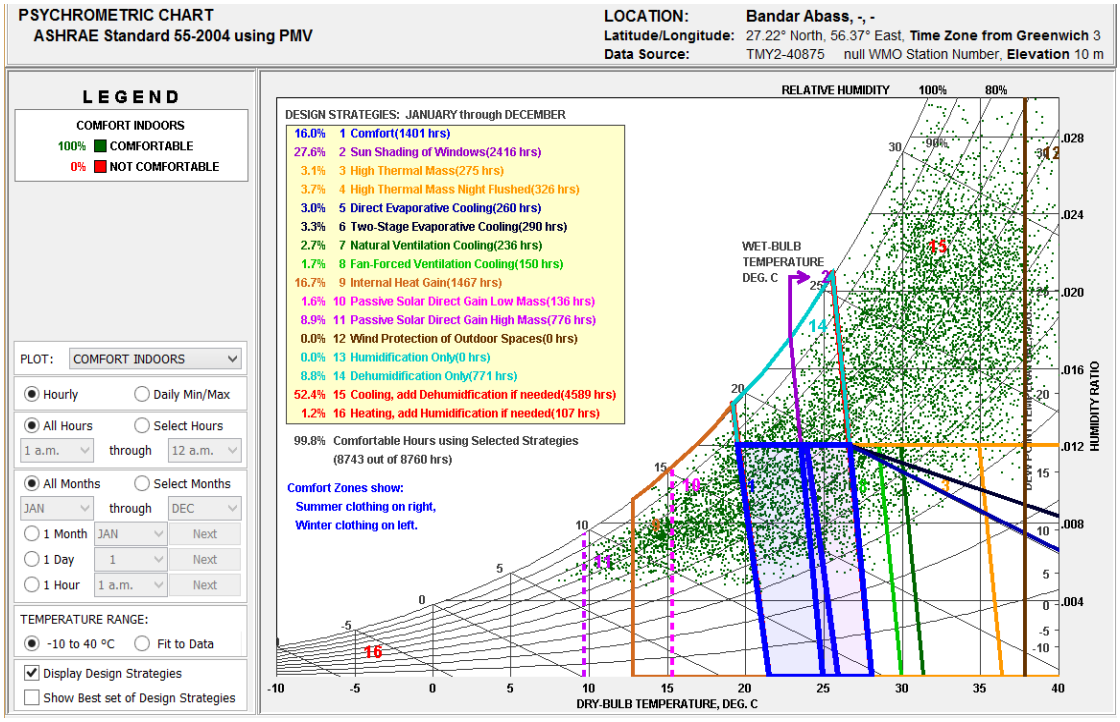

Fig. 18. The type of ACS proposed for Bandar Abbas city by the psychrometric chart.

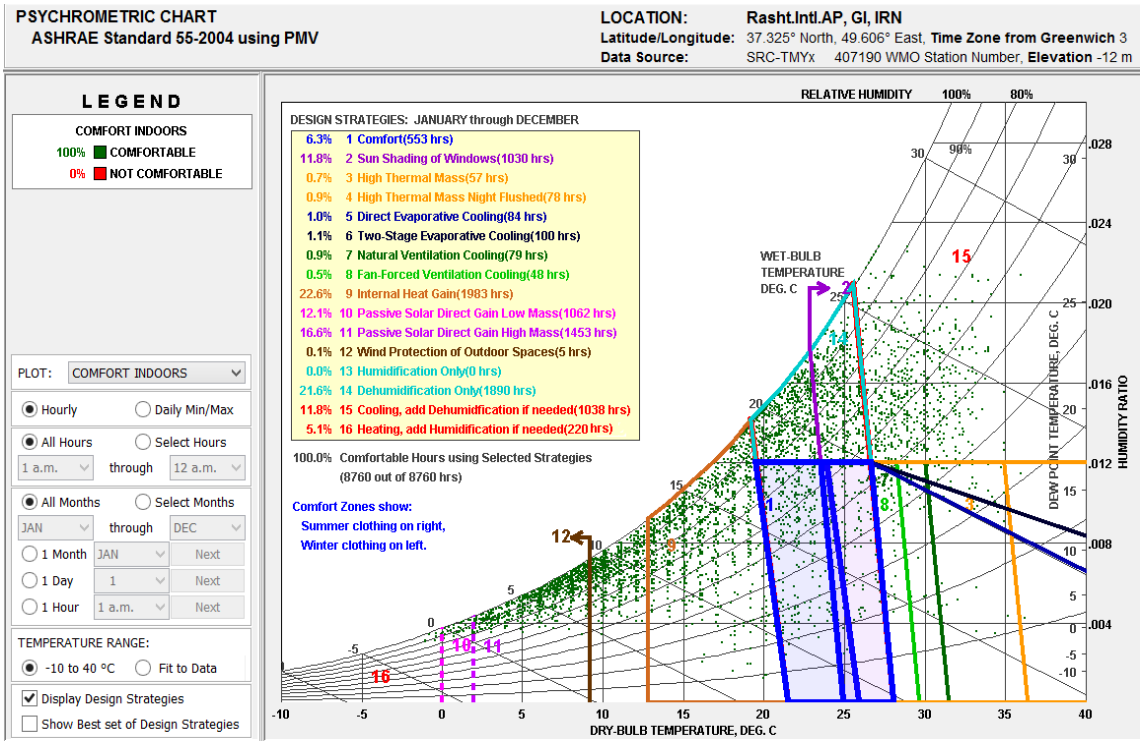

Fig. 19. The type of ACS proposed for Rasht city by the psychrometric chart.

5. Conclusions

In this study, the aim was to optimize the ACS in 4 different climates of Iran, and the following conclusions can be drawn from this study:

- The best ACS for Shahrekord and Tehran, due to the low air humidity and reducing the costs of paying bills, it is suitable to use an evaporative cooler for cooling and a radiator for heating. which have the proper CIACS in proportion to maintaining the PPD of the residents in

these areas.

- The best ACS for Bandar Abbas and Rasht, due to the high humidity in these cities and the need to use a cooling ACS in addition to reducing the cost of paying bills, is suitable for the VRF system for heating and cooling. This system has the best performance, in addition to lowering the CIACS and maintaining the PPD of the people inside the building.
- By examining different models and companies that manufacture all kinds of ACS, among 40 different types of ACS for the city of Tehran, the use of Mashhad Davam evaporative cooler and Eco radiator has the best performance for cooling and heating the building space according to their specified target functions.
- By examining different models and companies that manufacture all kinds of ACS, among 40 different types of ACS for Shahrekord city, the use of the Absal evaporative cooler and the Eco radiator has the best performance for cooling and heating the building space according to the target functions.
- By examining different models and companies that manufacture various types of ACS, among 40 different types of ACS for Bandar Abbas city, the use of the Boyman VRF system has the best performance for cooling and heating the building space according to the specified target functions.
- By examining different models and companies that manufacture various types of ACS, among 40 different types of ACS for the city of Rasht, the use of the VRF Green system has the best performance for cooling and heating the building space according to the specified target functions.

References

[1] Khoukhi, M., The combined effect of heat and moisture transfer dependent thermal conductivity of polystyrene insulation material: Impact on building energy performance. Energy and buildings, 2018. 169: p. 228-235.

[2] Fischedick, M., et al., Industry In: Climate Change 2014: Mitigation of Climate Change. Contribution of Working Group III to the Fifth Assessment Report of the Intergovernmental Panel on Climate Change. Technical Report. 2014.

[3] Marin, P., et al., Energy savings due to the use of PCM for relocatable lightweight buildings passive heating and cooling in different weather conditions. Energy and Buildings, 2016. 129: p. 274-283.

[4] Heubaum, H. and F. Biermann, Integrating global energy and climate governance: The changing role of the International Energy Agency. Energy Policy, 2015. 87: p. 229-239.

[5] 2023; Available from: https://www.bsria.com/uk/news/article/world-air-conditioning-market-grows-thanks-to-hot-spots/.

[6] Léger, J., et al., Comparing electric heating systems at equal thermal comfort: An experimental investigation. Building and Environment, 2018. 128: p. 161-169.

[7] Aktacir, M.A., O. Büyükalaca, and T. Yılmaz, A case study for influence of building thermal insulation on cooling load and air-conditioning system in the hot and humid regions. Applied Energy, 2010. 87(2): p. 599-607.

[8] Cen, C., et al., Experimental comparison of thermal comfort during cooling with a fan coil system and radiant floor system at varying space heights. Building and Environment, 2018. 141: p. 71-79.

[9] Pandelidis, D., et al., Performance study of a novel dew point evaporative cooler in the climate of central Europe using building simulation tools. Building and Environment, 2020. 181: p. 107101.

[10] Tewari, P., et al., Field study on indoor thermal comfort of office buildings using evaporative cooling in the composite climate of India. Energy and Buildings, 2019. 199: p. 145-163.

[11] Naderi, E., et al., Simulation-based performance analysis of residential direct evaporative coolers in four climate regions of Iran. Journal of Building Engineering, 2020. 32: p. 101514.

[12] Yu, X., et al., Comparative study of the cooling energy performance of variable refrigerant flow systems and variable air

volume systems in office buildings. Applied energy, 2016. 183: p. 725-736.
[13] Jiang, Y., T. Ge, and R. Wang, Performance simulation of a joint solid desiccant heat pump and variable refrigerant flow air conditioning system in EnergyPlus. Energy and buildings, 2013. 65: p. 220-230.
[14] Song, G.-S., J.-H. Lim, and T.-K. Ahn, Air conditioner operation behaviour based on students' skin temperature in a classroom. Applied ergonomics, 2012. 43(1): p. 211-216.
[15] Aynur, T.N., Y. Hwang, and R. Radermacher, Simulation comparison of VAV and VRF air conditioning systems in an existing building for the cooling season. Energy and Buildings, 2009. 41(11): p. 1143-1150.
[16] Moon, H.J. and S.H. Yang, Evaluation of the energy performance and thermal comfort of an air conditioner with temperature and humidity controls in a cooling season. HVAC&R Research, 2014. 20(1): p. 61-71.
[17] Zhang, R., et al., A novel Variable Refrigerant Flow (VRF) heat recovery system model: Development and validation. Energy and Buildings, 2018. 168: p. 399-412.
[18] Nada, S., et al., Experimental investigation of energy and exergy performance of a direct evaporative cooler using a new pad type. Energy and Buildings, 2019. 203: p. 109449.
[19] Chu, C.-M., T.-L. Jong, and Y.-W. Huang, Thermal comfort control on multi-room fan coil unit system using LEE-based fuzzy logic. Energy Conversion and Management, 2005. 46(9-10): p. 1579-1593.
[20] Bishoyi, D. and K. Sudhakar, Experimental performance of a direct evaporative cooler in composite climate of India. Energy and Buildings, 2017. 153: p. 190-200.
[21] Deshmukh, S., et al., Fault detection in commercial building VAV AHU: A case study of an academic building. Energy and Buildings, 2019. 201: p. 163-173.
[22] MARTíNEZ, P., et al., Experimental study on energy performance of a split air-conditioner by using variable thickness evaporative cooling pads coupled to the condenser. Applied Thermal Engineering, 2016. 105: p. 1041-1050.
[23] Tewari, P., et al., Advancing building bioclimatic design charts for the use of evaporative cooling in the composite climate of India. Energy and Buildings, 2019. 184: p. 177-192.
[24] Gheibi, A. and A. Rahmati, An experimental and numerical investigation on thermal performance of a new modified baseboard radiator. Applied Thermal Engineering, 2019. 163: p. 114324.
[25] Yun, G.Y., J.H. Lee, and H.J. Kim, Development and application of the load responsive control of the evaporating temperature in a VRF system for cooling energy savings. Energy and Buildings, 2016. 116: p. 638-645.
[26] Yildiz, A. and M.A. Ersöz, Determination of the economical optimum insulation thickness for VRF (variable refrigerant flow) systems. Energy, 2015. 89: p. 835-844.
[27] Krishnamoorthy, S. and M. Modera, Impacts of duct leakage on central outdoor-air conditioning for commercial-building VAV systems. Energy and Buildings, 2016. 119: p. 340-351.
[28] Yao, Y. and L. Wang, Energy analysis on VAV system with different air-side economizers in China. Energy and Buildings, 2010. 42(8): p. 1220-1230.
[29] Cho, Y.-H. and M. Liu, Minimum airflow reset of single duct VAV terminal boxes. Building and Environment, 2009. 44(9): p. 1876-1885.
[30] Baghoolizadeh, M., et al., Optimization of annual electricity consumption costs and the costs of insulation and phase change materials in the residential building using artificial neural network and genetic algorithm methods. Journal of Energy Storage, 2023. 62: p. 106916.
[31] Baghoolizadeh, M., et al., Using of artificial neural networks and different evolutionary algorithms to predict the viscosity and thermal conductivity of silica-alumina-MWCN/water nanofluid. Heliyon, 2024.
[32] Baghoolizadeh, M., et al., Multi-objective optimization of annual electricity consumption and annual electricity production of a residential building using photovoltaic shadings. International Journal of Energy Research: p. 1-45.
[33] Baghoolizadeh, M., et al., The effect of photovoltaic shading with ideal tilt angle on the energy cost optimization of a building

model in European cities. Energy for Sustainable Development, 2022. 71: p. 505-516.
[34] Baghoolizadeh, M., et al., Using different machine learning algorithms to predict the rheological behavior of oil SAE40-based nano-lubricant in the presence of MWCNT and MgO nanoparticles. Tribology International, 2023: p. 108759.
[35] Baghoolizadeh, M., et al., A prediction model for CO2 concentration and multi-objective optimization of CO2 concentration and annual electricity consumption cost in residential buildings using ANN and GA. Journal of Cleaner Production, 2022. 379: p. 134753.
[36] Baghoolizadeh, M., et al., Improving CO2 concentration, CO2 pollutant and occupants' thermal comfort in a residential building using genetic algorithm optimization. Energy and Buildings, 2023: p. 113109.
[37] Baghoolizadeh, M., et al., Multi-objective optimization of Venetian blinds in office buildings to reduce electricity consumption and improve visual and thermal comfort by NSGA-II. Energy and Buildings, 2022. 278: p. 112639.
[38] Baghoolizadeh, M., et al., A multi-objective optimization of a building's total heating and cooling loads and total costs in various climatic situations using response surface methodology. Energy Reports, 2021. 7: p. 7520-7538.
[39] Rostamzadeh-Renani, M., et al., The effect of canard's optimum geometric design on wake control behind the car using Artificial Neural Network and Genetic Algorithm. ISA transactions, 2022. 131: p. 427-443.
[40] Rostamzadeh-Renani, M., et al., The effect of vortex generators on the hydrodynamic performance of a submarine at a high angle of attack using a multi-objective optimization and computational fluid dynamics. Ocean Engineering, 2023. 282: p. 114932.
[41] Rostamzadeh-Renani, R., et al., Prediction of the thermal behavior of multi-walled carbon nanotubes-CuO-CeO2 (20-40-40)/water hybrid nanofluid using different types of regressors and evolutionary algorithms for designing the best artificial neural network modeling. Alexandria Engineering Journal, 2023. 84: p. 184-203.
[42] Rostamzadeh-Renani, R., et al., Multi-objective optimization of rheological behavior of nanofluids containing CuO nanoparticles by NSGA II, MOPSO, and MOGWO evolutionary algorithms and Group Method of Data Handling Artificial neural networks. Materials Today Communications, 2023: p. 107709.
[43] Jafari Ghahfarokhi, N., et al., Optimization of a novel micromixer with fan-shaped obstacles. Chemical Papers, 2024: p. 1-10.
[44] Hakimazari, M., et al., Multi-objective optimization of daylight illuminance indicators and energy usage intensity for office space in Tehran by genetic algorithm. Energy Reports, 2024. 11: p. 3283-3306.
[45] Rostamzadeh-Renani, M., et al., A multi-objective and CFD based optimization of roof-flap geometry and position for simultaneous drag and lift reduction. Propulsion and Power Research, 2024.
[46] Bayareh, M. and M. Baghoolizadeh, An overview of the magnetic field effect on heat transfer and entropy generation in cavities: Application of the second law of thermodynamics and artificial intelligence. International Communications in Heat and Mass Transfer, 2024. 151: p. 107238.
[47] Kerdan, I.G. and D.M. Gálvez, Artificial neural network structure optimisation for accurately prediction of exergy, comfort and life cycle cost performance of a low energy building. Applied Energy, 2020. 280: p. 115862.
[48] Markarian, E. and F. Fazelpour, Multi-objective optimization of energy performance of a building considering different configurations and types of PCM. Solar Energy, 2019. 191: p. 481-496.
[49] Kim, W., S.W. Jeon, and Y. Kim, Model-based multi-objective optimal control of a VRF (variable refrigerant flow) combined system with DOAS (dedicated outdoor air system) using genetic algorithm under heating conditions. Energy, 2016. 107: p. 196-204.
[50] Lee, J.M., et al., Application of artificial neural networks for optimized AHU discharge air temperature set-point and minimized cooling energy in VAV system. Applied Thermal Engineering, 2019. 153: p. 726-738.

[51] Xu, X., et al., A model-based optimal ventilation control strategy of multi-zone VAV air-conditioning systems. Applied Thermal Engineering, 2009. 29(1): p. 91-104.
[52] Baghoolizadeh, M., et al., Multi-objective optimization of Venetian blinds in office buildings to reduce electricity consumption and improve visual and thermal comfort by NSGA-II. Energy and Buildings, 2023. 278: p. 112639.
[53] Baghoolizadeh, M., et al., Improving CO2 concentration, CO2 pollutant and occupants' thermal comfort in a residential building using genetic algorithm optimization. Energy and Buildings, 2023. 291: p. 113109.
[54] Fathalian, A. and H. Kargarsharifabad, Actual validation of energy simulation and investigation of energy management strategies (Case Study: An office building in Semnan, Iran). Case studies in thermal engineering, 2018. 12: p. 510-516.
[55] Pourvahidi, P. and M.B. Ozdeniz, Bioclimatic analysis of Iranian climate for energy conservation in architecture. Scientific Research and Essays, 2013. 8(1): p. 6-16.
[56] Code No.19: Energy Efficiency Bureau for compiling and promoting National regulations for Buildings, Ministry of Housing and Urbanism. 2011: Tehran, Iran.
[57] National Building Code. Part 13 Design and Implementation of Electrical Installations for Buildings. 2009, Iran Building and Housing Research Center: Tehran, Iran.
[58] Iran radiator propertice. 2023; Available from: https://iranradiatorco.com/product-category/radiator/
[59] Butane radiator propertice. 2023; Available from: https://butaneindustrial.com/%d9%85%d8%ad%d8%b5%d9%88%d9%84%d8%a7%d8%aa/butane-products/radiators/.
[60] Evaporative cooler Mashhad Davam propertice 2023; Available from: https://afshinkala.ir/product/%da%a9%d9%88%d9%84%d8%b1-%d8%a2%d8%a8%db%8c-6500-%d9%85%d8%b4%d9%87%d8%af-%d8%af%d9%88%d8%a7%d9%85-md-6500/?utm_medium=PPC&utm_source=Torob.
[61] Evaporative cooler Absal propertice 2023; Available from: https://damapouya.com/product/%DA%A9%D9%88%D9%84%D8%B1-%D8%A2%D8%A8%DB%8C-%D8%A2%D8%A8%D8%B3%D8%A7%D9%84-%D9%85%D8%AF%D9%84-ac70.
[62] Cast iron boiler Shofajkar propertice 2023; Available from: https://tasisplus.ir/product-category/%d8%aa%d8%ac%d9%87%db%8c%d8%b2%d8%a7%d8%aa-%d9%85%d9%88%d8%aa%d9%88%d8%b1%d8%ae%d8%a7%d9%86%d9%87-%d9%88-%da%af%d8%b1%d9%85%d8%a7%db%8c%d8%b4%db%8c/%d8%a7%d9%86%d9%88%d8%a7%d8%b9-%d8%af%db%8c%da%af/%d8%af%db%8c%da%af-%d8%b4%d9%88%d9%81%d8%a7%da%98-%da%86%d8%af%d9%86%db%8c/mi3/.
[63] Cast iron boiler MI3 propertice 2023; Available from: https://damatajhiz.com/products/5937/%D8%AF%DB%8C%DA%AF-%DA%86%D8%AF%D9%86%DB%8C-%D8%B3%D9%88%D9%BE%D8%B1-200-%D8%B4%D9%88%D9%81%D8%A7%DA%98%DA%A9%D8%A7%D8%B1-4-%D9%BE%D8%B1%D9%87.
[64] Media air cooled chiller propertice. 2023; Available from: https://havasanj.ir/shop/hvac/%DA%86%DB%8C%D9%84%D8%B1-10-%D8%AA%D9%86-%D9%85%DB%8C%D8%AF%DB%8C%D8%A7-%D9%85%D8%AF%D9%84-mgb-d30w-rn1/
[65] Fan coil Green propertice. 2023; Available from: https://damatajhiz.com/products/3933/%D9%81%D9%86-%DA%A9%D9%88%DB%8C%D9%84-%D8%B2%D9%85%DB%8C%D9%86%DB%8C-%D8%AF%DA%A9%D9%88%D8%B1%D8%A7%D8%AA%DB%8C%D9%88-400cfm-%D8%AF%D9%85%D8%A7%D8%AA%D8%AC%D9%87%DB%8C%D8%B2-%D9%85%D8%AF%D9%84-dtgc400.

[66] Fan coil Goldiran ceiling propertice. 2023; Available from: https://damatajhiz.com/products/705/%D9%81%D9%86-%DA%A9%D9%88%DB%8C%D9%84-%D8%B3%D9%82%D9%81%DB%8C-%D8%AA%D9%88%DA%A9%D8%A7%D8%B1-%DA%AF%D9%84%D8%AF%DB%8C%D8%B1%D8%A7%D9%86-400cfm-%D9%85%D8%AF%D9%84-glkt3-400.

[67] Fan coil Goldiran casety propertice. 2023; Available from: https://damatajhiz.com/products/681/%D9%81%D9%86-%DA%A9%D9%88%DB%8C%D9%84-%DA%A9%D8%A7%D8%B3%D8%AA%DB%8C-%DB%8C%DA%A9-%D8%B7%D8%B1%D9%81%D9%87-%DA%AF%D9%84%D8%AF%DB%8C%D8%B1%D8%A7%D9%86-400cfm-%D9%85%D8%AF%D9%84-glkc-400.

[68] Fan coil G-Plus propertice. 2023; Available from: https://damatajhiz.com/products/5569/%D9%81%D9%86-%DA%A9%D9%88%DB%8C%D9%84-%D8%B3%D9%82%D9%81%DB%8C-%D8%AA%D9%88%DA%A9%D8%A7%D8%B1-%D8%AC%DB%8C-%D9%BE%D9%84%D8%A7%D8%B3-%D9%85%D8%AF%D9%84-gfu-lc400g30.

[69] Fan coil Media built-in ceiling propertice. 2023; Available from: https://damatajhiz.com/products/822/%D9%81%D9%86-%DA%A9%D9%88%DB%8C%D9%84-%D8%B3%D9%82%D9%81%DB%8C-%D8%AA%D9%88%DA%A9%D8%A7%D8%B1-%D9%85%DB%8C%D8%AF%DB%8C%D8%A7-%D8%A8%D8%A7-%DA%A9%D9%88%DB%8C%D9%84-%D8%B3%D9%87-%D8%B1%D8%AF%DB%8C%D9%81%D9%87-%D9%85%D8%AF%D9%84-mkt3-400.

[70] Fan coil Media ground propertice. 2023; Available from: https://damatajhiz.com/products/748/%D9%81%D9%86%DA%A9%D9%88%DB%8C%D9%84-%D8%B2%D9%85%DB%8C%D9%86%DB%8C-%D9%85%DB%8C%D8%AF%DB%8C%D8%A7-400cfm-%D9%85%D8%AF%D9%84-mkf-400.

[71] Fan coil Media casety propertice. 2023; Available from: https://damatajhiz.com/products/815/%D9%81%D9%86-%DA%A9%D9%88%DB%8C%D9%84-%DA%A9%D8%A7%D8%B3%D8%AA%DB%8C-%DB%8C%DA%A9-%D8%B7%D8%B1%D9%81%D9%87-%D9%85%DB%8C%D8%AF%DB%8C%D8%A7-%D9%85%D8%AF%D9%84-mkc-400.

[72] Fan coil Saran propertice. 2023; Available from: https://damatajhiz.com/products/3305/%D9%81%D9%86-%DA%A9%D9%88%DB%8C%D9%84-%D8%B2%D9%85%DB%8C%D9%86%DB%8C-%D9%85%D9%88%D8%B1%D8%A8-%D8%B2%D9%86-%D8%B3%D8%A7%D8%B1%D8%A7%D9%86-srfcse-200.

[73] Fan coil DamaTajhiz propertice. 2023; Available from: https://damatajhiz.com/products/4481/%D9%81%D9%86-%DA%A9%D9%88%DB%8C%D9%84-%D8%B3%D9%82%D9%81%DB%8C-%D8%AA%D9%88%DA%A9%D8%A7%D8%B1-%DA%AF%D8%B1%DB%8C%D9%86-%D9%85%D8%AF%D9%84-gdf600p1.

[74] PTHP IRAN RADIATOR propertice. 2023; Available from: https://iranradiatorco.com/product/split-9000-xa-a/.

[75] PTHP TRUST propertice. 2023; Available from: https://damapouya.com/%DA%A9%D9%88%D9%84%D8%B1-%DA%AF%D8%A7%D8%B2%DB%8C-%D8%A7%D8%B3%D9%BE%D9%84%DB%8C%D8%AA-%D8%AA%D8%B1%D8%A7%D8%B3%D8%AA/trust-9000-inverter-ac.html.

[76] PTHP HOMAX propertice. 2023; Available from: https://damapouya.com/%DA%A9%D9%8

8%D9%84%D8%B1-%DA%AF%D8%A7%D8%B2%DB%8C-%D8%A7%D8%B3%D9%BE%D9%84%DB%8C%D8%AA-%D9%87%D9%88%D9%85%DA%A9%D8%B3/%DA%A9%D9%88%D9%84%D8%B1-%DA%AF%D8%A7%D8%B2%DB%8C-%D9%87%D9%88%DA%A9%D8%B3-9000-%D8%B3%D8%B1%D8%AF-%D9%88-%DA%AF%D8%B1%D9%85.html.

[77] PTHP Gary propertice. 2023; Available from: https://damapouya.com/product/%DA%A9%D9%88%D9%84%D8%B1-%DA%AF%D8%A7%D8%B2%DB%8C-%DA%AF%D8%B1%DB%8C-9000-r4matic-%D8%B3%D8%B1%D8%AF-%D9%88-%DA%AF%D8%B1%D9%85.

[78] PTHP GREEN 9000 propertice. 2023; Available from: https://damapouya.com/%DA%A9%D9%88%D9%84%D8%B1-%DA%AF%D8%A7%D8%B2%DB%8C-%D8%A7%D8%B3%D9%BE%D9%84%DB%8C%D8%AA-%DA%AF%D8%B1%DB%8C%D9%86/%DA%A9%D9%88%D9%84%D8%B1%DA%AF%D8%A7%D8%B2%DB%8C-9000-%DA%AF%D8%B1%DB%8C%D9%86.html.

[79] PTHP HYUNDAI 9000 model 0930W propertice. 2023; Available from: https://damapouya.com/%DA%A9%D9%88%D9%84%D8%B1-%DA%AF%D8%A7%D8%B2%DB%8C-%D8%A7%D8%B3%D9%BE%D9%84%DB%8C%D8%AA-%D9%87%DB%8C%D9%88%D9%86%D8%AF%D8%A7%DB%8C/%DA%A9%D9%88%D9%84%D8%B1-%DA%AF%D8%A7%D8%B2%DB%8C-%D9%87%DB%8C%D9%88%D9%86%D8%AF%D8%A7%DB%8C-%D8%A7%DB%8C%D9%86%D9%88%D8%B1%D8%AA%D8%B1-9000-%D8%B3%D8%B1%D8%AF-%D9%88-%DA%AF%D8%B1%D9%85.html.

[80] PTHP HYUNDAI 9000 model 0932WT1 propertice. 2023; Available from: https://damapouya.com/%DA%A9%D9%88%D9%84%D8%B1-%DA%AF%D8%A7%D8%B2%DB%8C-%D8%A7%D8%B3%D9%BE%D9%84%DB%8C%D8%AA-%D9%87%DB%8C%D9%88%D9%86%D8%AF%D8%A7%DB%8C/%DA%A9%D9%88%D9%84%D8%B1-%DA%AF%D8%A7%D8%B2%DB%8C-%D9%87%DB%8C%D9%88%D9%86%D8%AF%D8%A7%DB%8C-9000-%D8%B3%D8%B1%D8%AF-%D9%88-%DA%AF%D8%B1%D9%85.html.

[81] PTHP GREEN 24000 propertice. 2023; Available from: https://emalls.ir/%d9%85%d8%b4%d8%ae%d8%b5%d8%a7%d8%aa_%da%a9%d9%88%d9%84%d8%b1-%da%af%d8%a7%d8%b2%db%8c-24000-%da%af%d8%b1%db%8c%d9%86-%d9%85%d8%af%d9%84-GSW-H24P1T1-R1~id~1302225.

[82] PTHP General Gold propertice. 2023; Available from: https://emalls.ir/%d9%85%d8%b4%d8%ae%d8%b5%d8%a7%d8%aa_GG-S24000-Platinum~id~4507093.

[83] PTHP PAKSHOMA propertice. 2023; Available from: https://emalls.ir/%d9%85%d8%b4%d8%ae%d8%b5%d8%a7%d8%aa_%da%a9%d9%88%d9%84%d8%b1-%da%af%d8%a7%d8%b2%db%8c-%d9%be%d8%a7%da%a9%d8%b4%d9%88%d9%85%d8%a7-%d9%85%d8%af%d9%84-MPF-24CH~id~5075253.

[84] PTHP KAZUKI propertice. 2023; Available from: https://damatajhiz.com/products/8321/%DA%A9%D9%88%D9%84%D8%B1-%DA%AF%D8%A7%D8%B2%DB%8C-%DA%A9%D8%A7%D8%B2%D9%88%DA%A9%DB%8C-24000-%D9%85%D8%AF%D9%84-iac-24chxaa.

[85] PTHP PAKSHOMA 24000 propertice. 2023; Available from: https://damatajhiz.com/products/8208/%DA%A9%D9%88%D9%84%D8%B1-%DA%AF%D8%A7%D8%B2%DB%8C-%D8%B3%D8%B1%D8%AF-24000-%D9%BE%D8%A7%DA%A9%D8%B4%D9%88%D9%85%D8%A7-mpr-24c.

[86] PTAC LG. 2023; Available from: https://store.directsupply.com/Product/direc

t-supply-ptac-heat-pump-9-000-btu-230-208v-20-amp-4756807?quantity=1&.

[87] PTAC Direct supply. 2023; Available from: https://ptac4less.com/new-lg-9000-btu-ptac-air-conditioner-230-volt-20-amp-with-digital-controls-and-heat-pump.

[88] VRF external units HISENSE. 2023; Available from: https://leotahvieh.ir/%D8%B3%DB%8C%D8%B3%D8%AA%D9%85-%D9%85%D8%B1%DA%A9%D8%B2%DB%8C-vrf-%D9%87%D8%A7%DB%8C%D8%B3%D9%86%D8%B3/2797-%DB%8C%D9%88%D9%86%DB%8C%D8%AA-%D8%AE%D8%A7%D8%B1%D8%AC%DB%8C-avwt-76hkss.html.

[89] VRF external units BOYMAN. 2023; Available from: https://leotahvieh.ir/%D8%B3%DB%8C%D8%B3%D8%AA%D9%85-%D9%85%D8%B1%DA%A9%D8%B2%DB%8C-vrf-%D8%A8%D9%88%DB%8C%D9%85%D9%86/2307-%DB%8C%D9%88%D9%86%DB%8C%D8%AA-%D8%AE%D8%A7%D8%B1%D8%AC%DB%8C-22kw.html.

[90] VRF external units GREEN. 2023; Available from: https://leotahvieh.ir/%D8%B3%DB%8C%D8%B3%D8%AA%D9%85-%D9%85%D8%B1%DA%A9%D8%B2%DB%8C-vrf-%DA%AF%D8%B1%DB%8C%D9%86/2328-%DB%8C%D9%88%D9%86%DB%8C%D8%AA-%D8%AE%D8%A7%D8%B1%D8%AC%DB%8C-90000.html.

[91] VRF internal units HISENSE. 2023; Available from: https://leotahvieh.ir/%D8%B3%DB%8C%D8%B3%D8%AA%D9%85-%D9%85%D8%B1%DA%A9%D8%B2%DB%8C-vrf-%D9%87%D8%A7%DB%8C%D8%B3%D9%86%D8%B3/2808-%DB%8C%D9%88%D9%86%DB%8C%D8%AA-%D8%AF%D8%A7%D8%AE%D9%84%DB%8C-%D8%AF%DB%8C%D9%88%D8%A7%D8%B1%DB%8C-avs-22-urcsaba.html.

[92] VRF internal units BOYMAN. 2023; Available from: https://leotahvieh.ir/%D8%B3%DB%8C%D8%B3%D8%AA%D9%85-%D9%85%D8%B1%DA%A9%D8%B2%DB%8C-vrf-%D8%A8%D9%88%DB%8C%D9%85%D9%86/2323-%DB%8C%D9%88%D9%86%DB%8C%D8%AA-%D8%AF%D8%A7%D8%AE%D9%84%DB%8C-%D8%AF%DB%8C%D9%88%D8%A7%D8%B1%DB%8C-24000.html.

[93] VRF internal units GREEN. 2023; Available from: https://leotahvieh.ir/%D8%B3%DB%8C%D8%B3%D8%AA%D9%85-%D9%85%D8%B1%DA%A9%D8%B2%DB%8C-vrf-%DA%AF%D8%B1%DB%8C%D9%86/2348-%DB%8C%D9%88%D9%86%DB%8C%D8%AA-%D8%AF%D8%A7%D8%AE%D9%84%DB%8C-%D8%AF%DB%8C%D9%88%D8%A7%D8%B1%DB%8C-24000.html.

[94] The cost of gas bills. 2023; Available from: https://www.nigc-gl.ir/fa/Cshow17079.aspx.

[95] The cost of water bills. 2023; Available from: https://irandama.ir/%D8%B1%D8%A7%D9%87%D9%86%D9%85%D8%A7%DB%8C-%D9%85%D8%AD%D8%A7%D8%B3%D8%A8%D9%87-%D8%A2%D8%A8-%D8%A8%D9%87%D8%A7-%D8%AF%D8%B1-%D9%82%D8%A8%D9%88%D8%B6-%D8%B4%D8%B1%DA%A9%D8%AA-%D8%A2%D8%A8%D9%81%D8%A7/

[96] The cost of electricity bills. 2023.